

NASA TM X-55596

# NON-DISPERSIVE X-RAY EMISSION ANALYSIS FOR LUNAR SURFACE GEOCHEMICAL EXPLORATION

BY

J. I. TROMBKA  
I. ADLER  
R. SCHMADEBECK  
R. LAMOTHE

GPO PRICE \$ \_\_\_\_\_

CFSTI PRICE(S) \$ 2.50

AUGUST 1966

Hard copy (HC) \_\_\_\_\_

Microfiche (MF) .75

ff 653 July 65



GODDARD SPACE FLIGHT CENTER

GREENBELT, MD.

N67 13225

(ACCESSION NUMBER)

(PAGES)

(NASA CR OR TMX OR AD NUMBER)

(THRU)

(CODE)

(CATEGORY)

X-641-66-344

NON-DISPERSIVE X-RAY EMISSION ANALYSIS FOR  
LUNAR SURFACE GEOCHEMICAL EXPLORATION

by

J. I. Trombka, I. Adler,  
R. Schmadebeck and R. Lamothe

August 1966

Goddard Space Flight Center  
Greenbelt, Maryland

NON-DISPERSIVE X-RAY EMISSION ANALYSIS FOR  
LUNAR SURFACE GEOCHEMICAL EXPLORATION

by

J. I. Trombka and I. Adler

Goddard Space Flight Center

and

R. Schmadebeck and R. Lamothe

Melpar, Inc.

## I. INTRODUCTION

Our laboratory is presently investigating possible instrumentation for geochemical exploration of lunar or planetary surfaces for both manned and unmanned missions. The studies presently going forward will hopefully be used to define a total system having as its objectives: (1) obtaining operational numbers to help an astronaut in sample selection, and (2) obtaining geochemical information for mapping and preliminary surface analysis for manned and unmanned missions.

During the NASA 1965 Summer Conference on Lunar Exploration and Science, a considerable amount of attention was given by the Geochemistry Working Group to problems of surface exploration. While it was the consensus that the lunar environment was not particularly conducive to performing detailed geochemical analysis, there was, however, a great need for diagnostic tools to help the astronaut in selecting samples to be returned to earthside laboratories for comprehensive studies.

Consideration of diagnostic tools in relationship to the mission's objectives leads to a number of requirements that must be satisfied. These requirements range from geochemical parameters to be tested, optimum instruments to be employed and the vital problem of data acquisition and processing in very real time. Additionally, although the proposed instrumentation would primarily enable the astronaut to make decisions about sample selection, the design is sufficiently flexible to be useful for either manned or unmanned missions.

There are certain obvious characteristics that such instrumentation must meet such as small size and weight, reliability, stability and specificity. Because some of these requirements are at least in part conflicting, one must-

accept some tradeoffs. In the paper that follows one such instrument will be described as well as a computer program for data reduction.)

#### A. Instrumentation

Obviously, instrumental and system design is strictly determined by the mission profile. If, for example, one established a criterion that the probe is needed to help an astronaut in sample selection, by permitting him to perform relatively simple "in situ" analysis, then "non-dispersive" x-ray emission\* analysis becomes attractive. Such a device lends itself to portability as well as simple and rugged construction having minimal space and power requirements. In fact, such instrumentation has been proposed by a number of investigators such as Metzger, et al.<sup>1</sup>, Sellers and Ziegler<sup>2</sup>, and Kartunnen, et al.<sup>3</sup>, Trombka and Adler<sup>4</sup>. One of the most desirable features of such instrumentation is that x-ray spectra can be effectively excited by means of radioactive isotopic sources. The use of this type excitation has been discussed in a number of publications by Rhodes<sup>5</sup>, Cameron and Rhodes<sup>6</sup>, Robert<sup>7</sup>, Friedman<sup>8</sup>, Robert and Martinelli<sup>9</sup>, Inamura, et al.<sup>10</sup>. Most applications have involved the use of gamma, beta or bremsstrahlung sources but only recently has a systematic study of alpha excitation been undertaken.\*\*

The advantages of alpha particle excitation will be discussed in additional detail below.

In the program to be described attention has been directed to the common rock forming elements such as Mg, Al, Si, K, Ca and Fe. The characteristic K

---

\*The term non-dispersive is actually a misnomer. This expression which is in common usage means simply pulse height analysis as opposed to Bragg-Crystal dispersion.

\*\*See References 2, 7, 8, 10.

x-rays emitted by the majority of these elements may be classed as soft x-rays and, with the exception of Fe, range from 3A to approximately 12A. In this range one encounters problems of excessive absorption in the detector windows as well as low fluorescence yields. The instrument therefore requires an efficient design with emphasis on optimum excitation and geometry. It is also essential to use the thinnest detector windows compatible with mechanical strength and low counter gas leakage. An additional but very important requirement is to obtain the best possible detector resolution.

Figure 1 shows the rather simple instrumentation used in the laboratory\* for analysis. The apparatus consists of a radioactive source, a means for holding the sample, a proportional detector and an inlet for introducing helium into the chamber. Although a modest vacuum is desirable, helium is used at present in order to preserve the integrity of the alpha source window.

The samples to be analyzed may be introduced as powders, briquets or small flat sections of rock. The various components of the instrumentation will now be examined more closely.

### B. Excitation Sources

The obvious advantage in using radio-isotopes for exciting x-rays is that the source is small, requires no power and is the ultimate in reliability. It has already been amply demonstrated that radioactive sources of relatively low output will generate very adequate x-ray spectra in time periods as short as minutes.

Various types of isotopes have been found useful for x-ray emission analyses. These are beta sources, bremsstrahlung sources, K capture x-ray sources, and

---

\*This is not proposed as a flight instrument but is rather a breadboard for laboratory evaluation of the technique.

$\alpha$  SOURCE X-RAY ANALIZER

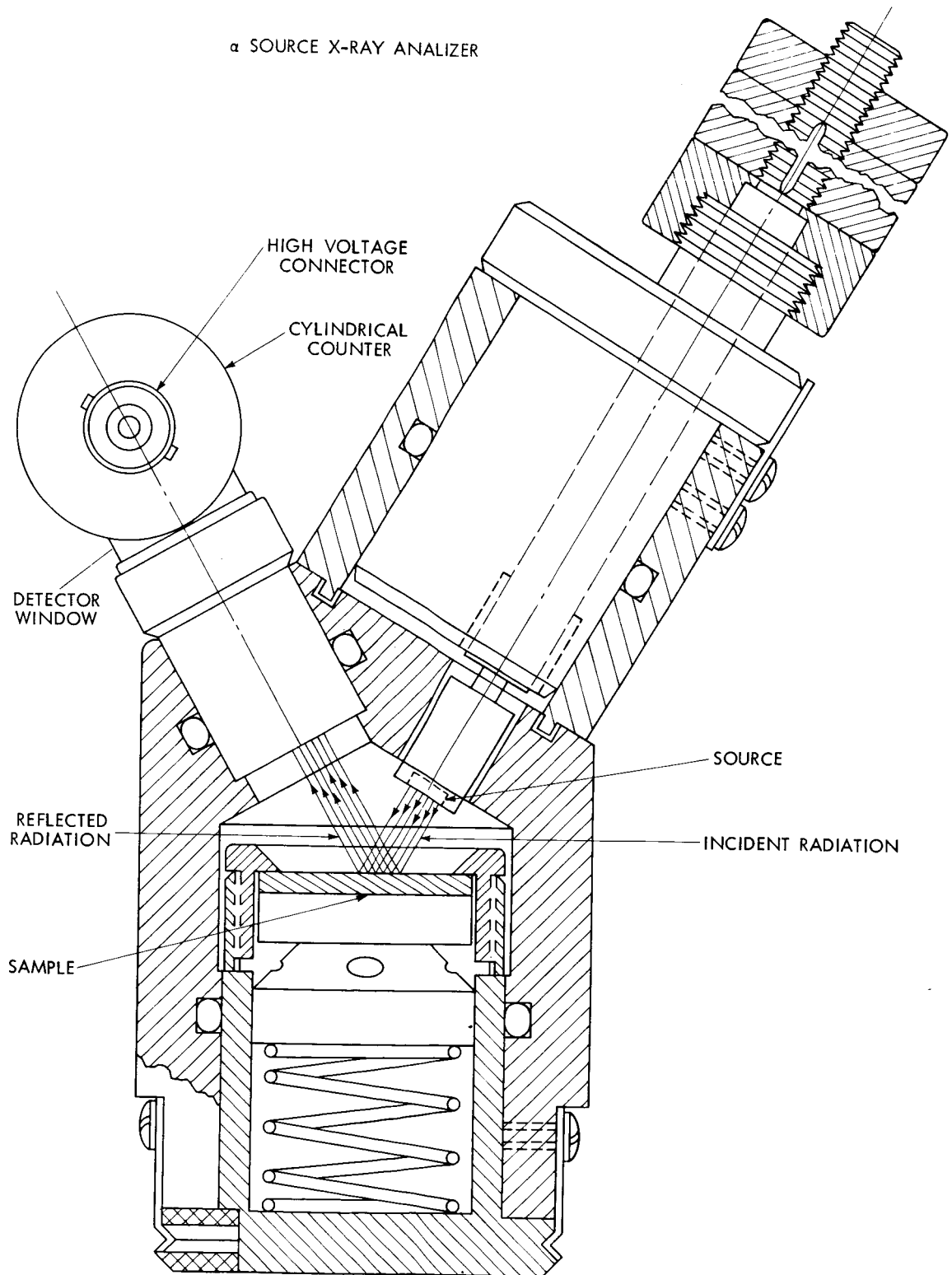


Figure 1

alpha emitters. It has been shown by Sellers and Ziegler<sup>2</sup> that alpha sources are particularly useful for light element analysis. These advantages can be tabulated as follows:

1. The cross section for ionization of the K x-rays increases approximately as  $1/Z^{12}$ . Thus the rapidly increasing ionization cross section with decreasing atomic number more than compensates for the decreasing fluorescence yield.
2. In comparison to electron excitation the alpha bremsstrahlung produced continuum is reduced by a factor of  $(m/M)^2$  where m and M are, respectively, the masses of the electron and alpha particles. As a consequence the continuum is reduced by a factor of about  $10^6$  to  $10^7$ .
3. Although alpha emission is usually associated with gamma ray emission it is possible to select nuclides where the gamma emission is both a small fraction of the alpha emission and the gamma rays are sufficiently removed from the excited x-rays to be easily discriminated against.
4. It is possible to obtain sources of high specific activity emitting very energetic alpha particles having energies of 4 to 6 mev such as  $\text{Po}^{210}$  and  $\text{Cm}^{242}$ .

While the advantages listed above make alpha emitters attractive sources for light element analysis there are a number of problems encountered in practice. Alpha sources are a serious potential health hazard and must be handled with extreme care. Because of the phenomenon of aggregate recoil, one should work either with sealed sources or in adequately ventilated hoods or glove boxes. As yet it is difficult to obtain sealed sources that can be operated in vacuum without using windows of such thickness as to seriously degrade the



energy of the emitted alpha particles. In the work to be described here measurements were made in helium at atmospheric pressure. The source holder is shown in Figure 2. The  $\text{Cm}^{242}$  source was approximately 15 mc deposited by coating on a stainless steel foil. The window in this instance was 0.0005 inch aluminum. Although no direct measurement of the energy distribution of the alpha particles was made, it was estimated that the effect of the window and helium atmosphere reduced the 6 mev alphas about 3 mev with an associated broadening of the energy peak.

Although it is true that alpha bombardment excites virtually no bremsstrahlung, one must expect some background. This background may come from the source container as well as x-rays excited by processes such as internally converted gamma rays and due to contaminating radioactive species. Figure 3 shows the background radiation from the  $\text{Cm}^{242}$  source scattered from a plastic sample. One can identify at the very least an AlK line from the source window, an FeK line from the substrate on which the  $\text{Cm}^{242}$  is deposited, a W line from the hevi-met (sintered W) container, as well as lines in the 13-18 kev region which may be attributed to the daughter product Pu as well as other contaminants.

### C. Detector

A major problem in light element analysis is associated with detection. The ideal would be a windowless detector with high efficiency and resolution. This is unfortunately beyond the state of the art at this time, particularly in the region of from 7 to 1 kev. The best detector available at this time is the thin window proportional counter, either flow or sealed. In the case of flow counters one can work easily with 0.001 inch Be or 0.00025 inch mylar. Figure 4 shows a typical

$\alpha$  EMITTER SOURCE HOLDER

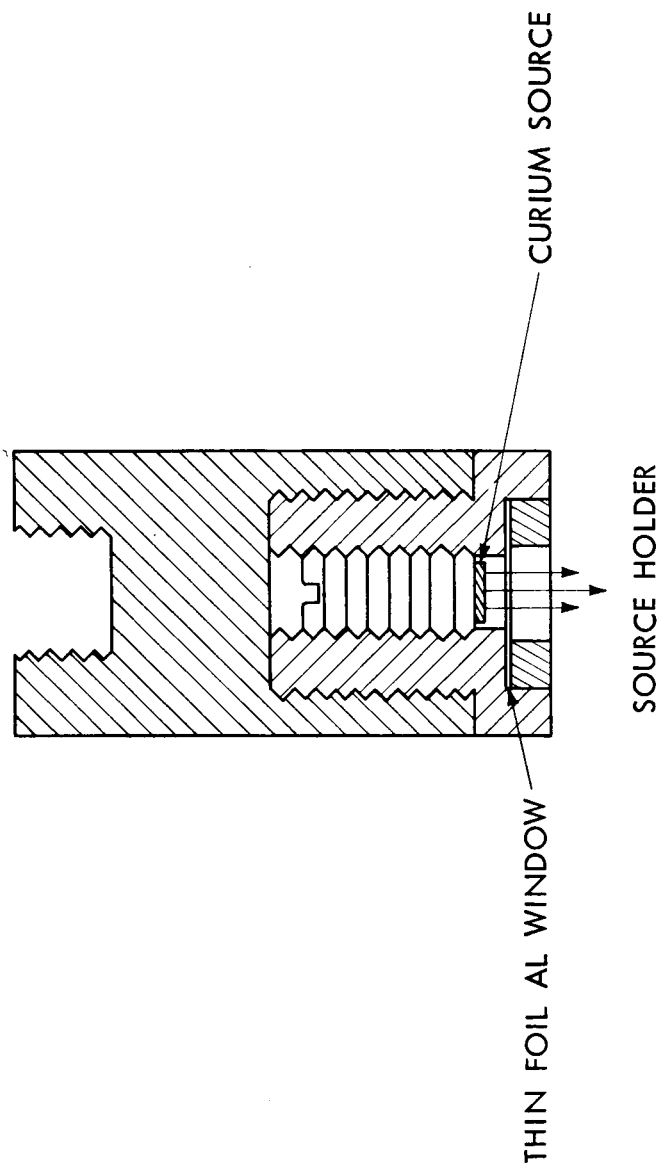


Figure 2

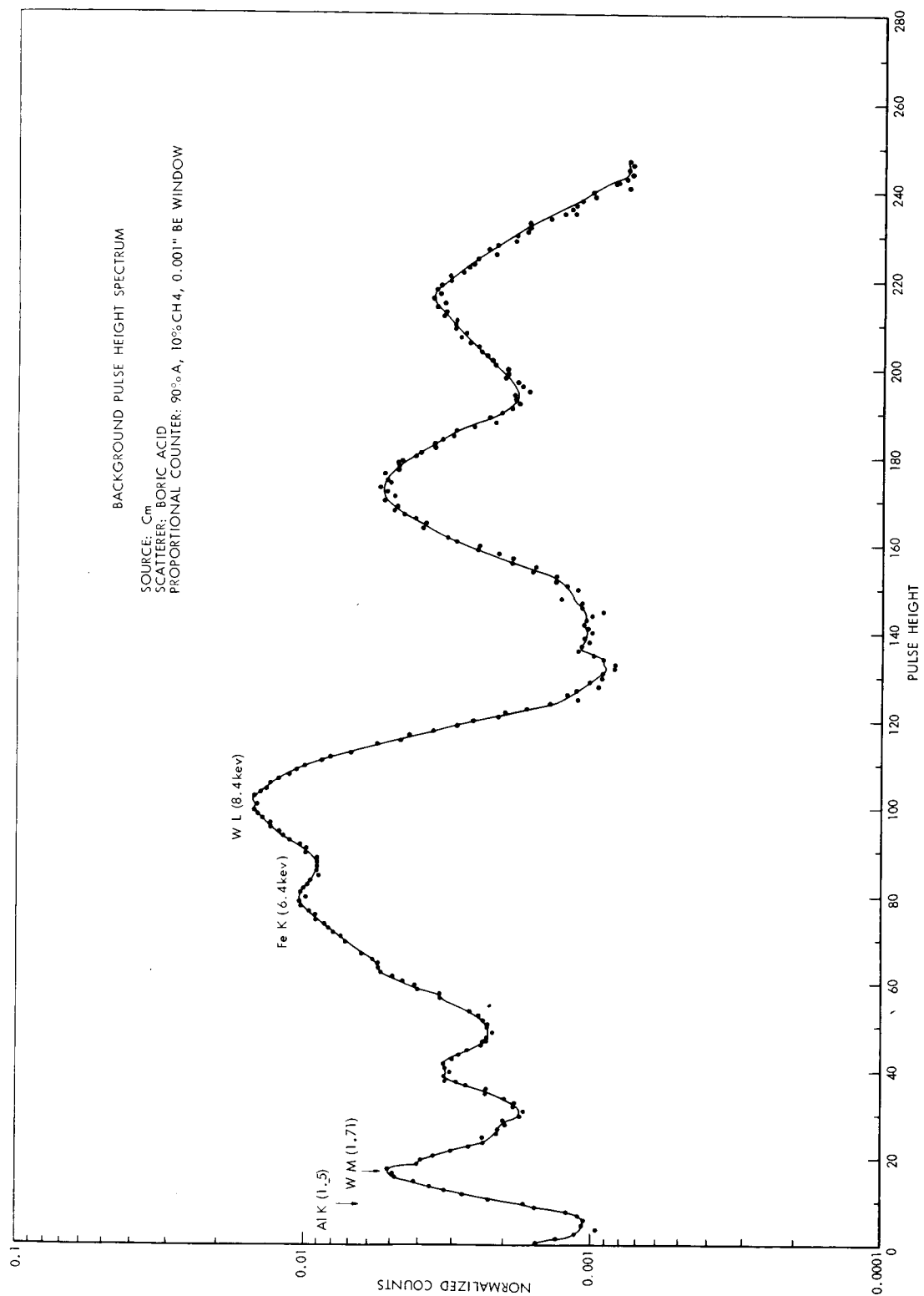


Figure 3

efficiency curve for a 2 cm detector using an Argon-methane mixture. This curve represents the product of window transmission and gas absorption. It can be seen that counter efficiency drops to about 10% at 11 A. When one combines this with phenomenon with the low fluorescence yield for the low Z elements, then the high ionization cross section of the alpha particles becomes particularly significant. The detector resolution used in this study was of the order of 17% for Fe<sup>55</sup>.

#### D. Electronics

This electronic arrangement was conventional consisting of a charge sensitive preamplifier feeding a high quality multi-channel analyzer. Although greater capabilities were available, 256 channels of the analyzer were found to be sufficient. Data readout was on perforated tapes which were then converted to punch cards for computer processing.

## II. DATA ANALYSIS

### A. Analytical Approach

In the previous section, the design of the X-ray emission system was shown to be greatly influenced by the mission objectives. Similarly, the analytical method is also closely related to these objectives. Methods can be developed for analysis of the measured spectra which at one extreme can compare spectral patterns and at the other extreme decompose the observed spectrum into mono-elemental components for detailed analysis. The simpler pattern recognition techniques are now being investigated for their possible application to problems involving sample selection, but since in almost all cases the more detailed analysis will be required, we will address ourselves to this problem.

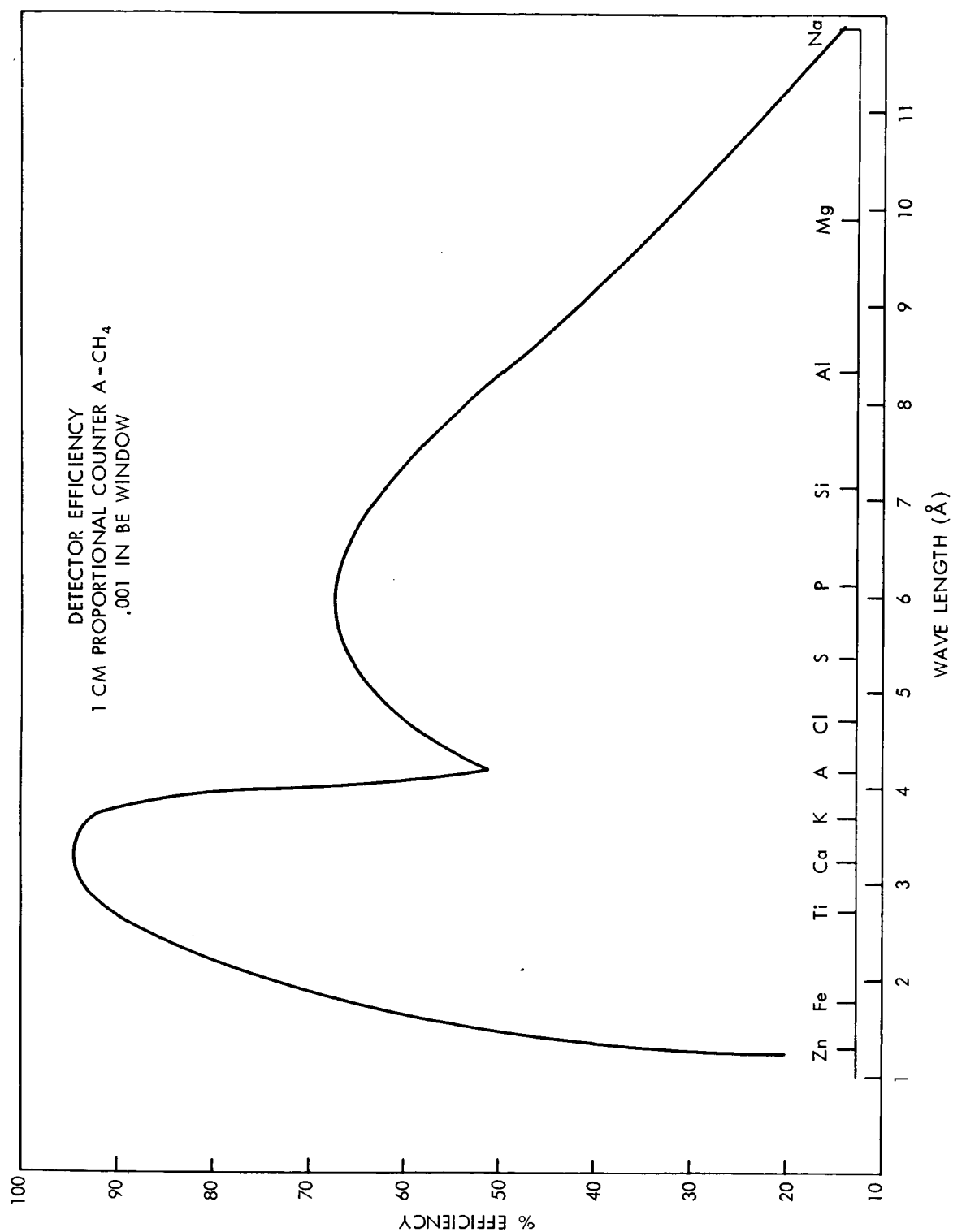


Figure 4

The problem of determining qualitative and quantitative information from a non-dispersive measurement of the x-ray emission can be divided into two parts. First, the differential x-ray energy spectrum (true energy spectrum incident upon the proportional counter) must be determined from the measured pulse height spectrum. The second step is then to deduce the chemical composition of the irradiated sample from the differential energy x-ray spectrum. The first step will be described in detail in this paper, and possible methods for performing the second step will be discussed by example at the end of this section.

### B. Nature of the Pulse Height Spectrum

We shall begin by defining what is meant by a pulse height spectrum. Consider the case of an ideal spectrometer looking at the Fe K spectrum, consisting of a number of monochromatic energies. We would observe a spectral distribution consisting of a number of discrete lines as shown in Figure 5. If, in practice, the x-ray energies are examined by means of a proportional counter detector and a pulse height analyzer, the spectrum becomes a continuous distribution as shown in Figure 5. Here we see the effect of instrumental smearing due to such factors as resolution, a statistical fluctuation in the detection process, detector geometry, electronic noise, etc. In many cases the spectrum is further complicated by an escape peak phenomenon due to partial absorption of the incident energies. It is obvious that any program of reducing a pulse height distribution to pulse height energies must concern itself with and remove these instrumental factors. This necessary approach will now be discussed in some detail.

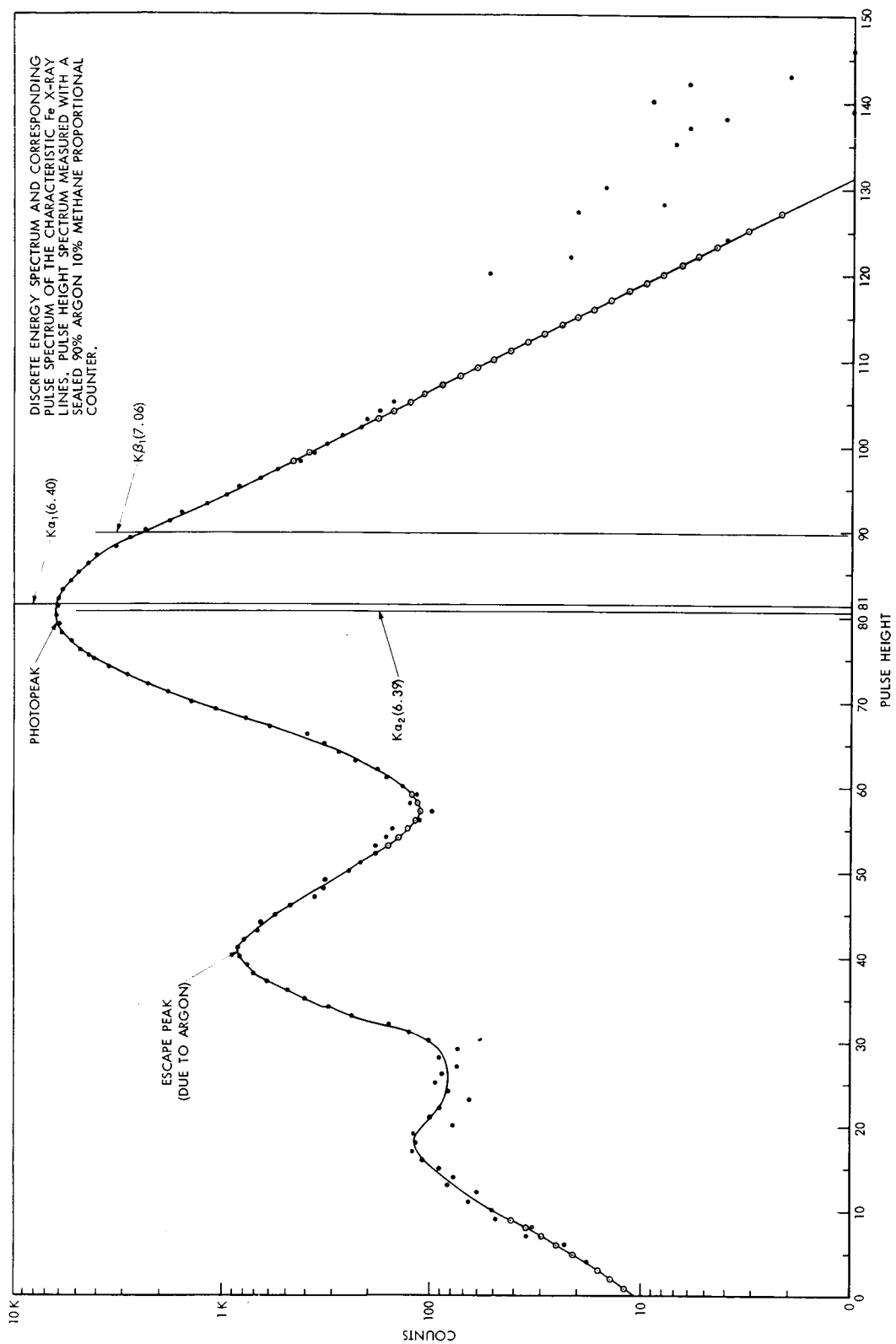


Figure 5

It has been observed that the x-ray photopeaks show a nearly Gaussian distribution and that the resolution of the peaks is a function of energy, the resolution  $R$  being defined as

$$R = \frac{W_{1/2}}{P_m}, \quad (1)$$

where  $W_{1/2}$  is the width of the photopeak at half the maximum amplitude, and  $P_m$  is the position of the pulse height maximum, where the width and peak are expressed in the same units (energy or channel window). The resolution is inversely proportional to some power of the pulse height or energy

$$R \sim E^{-n} \quad (2)$$

Theoretically<sup>11</sup>  $n = 0.5$  although experimentally  $n$  is usually greater or equal to 0.5. In the cases we have examined,  $n$  has varied from 0.5 to 0.67 and appears to be affected by the resolution of a given detector.

If one irradiates a mixture of elements with alpha particles and records the pulse height spectrum, the total observed polyelemental spectrum will be made up of a summation of the monoelemental components as shown in Figure 6.

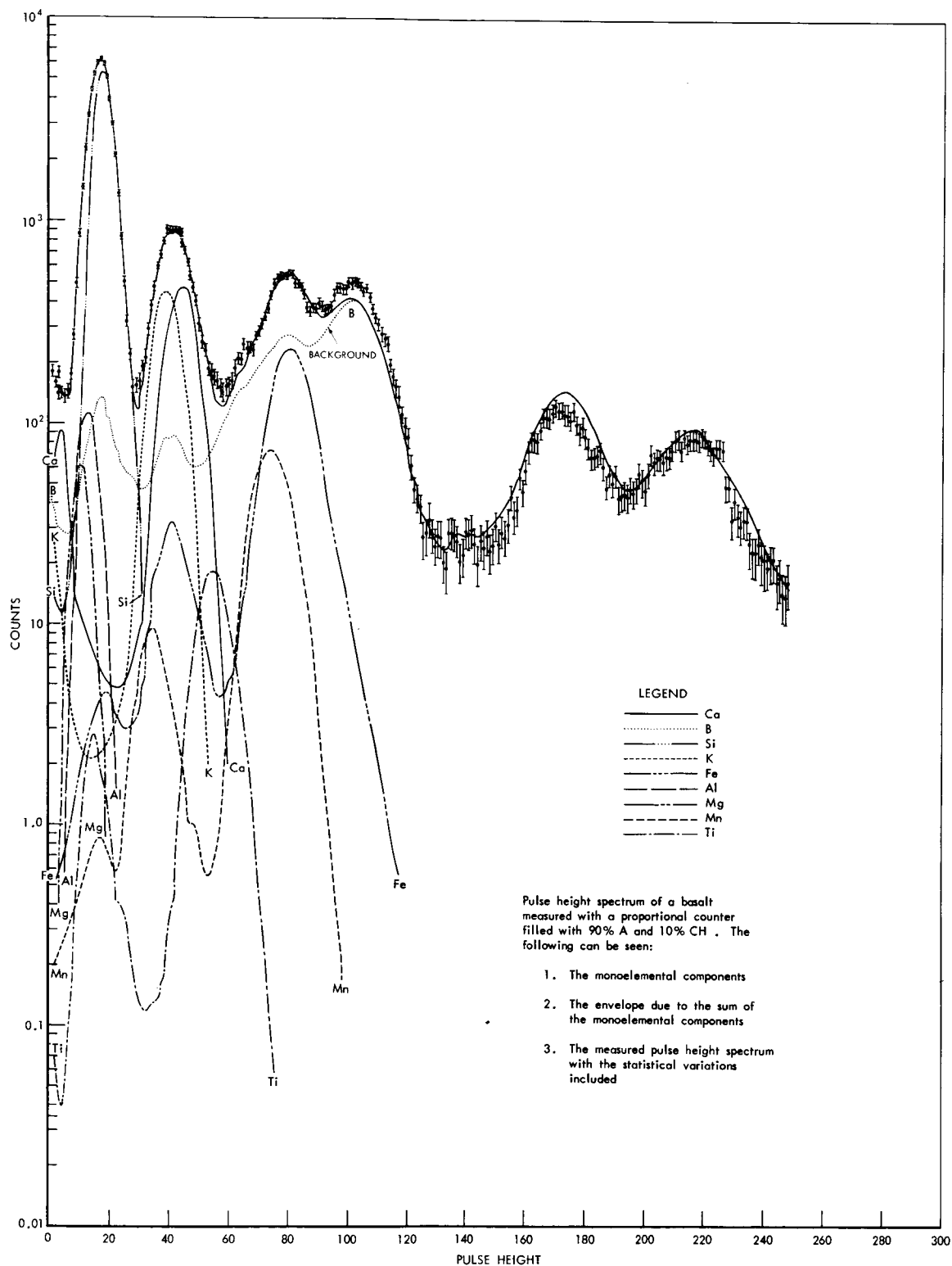
If  $\rho_i$  is taken as the measured count in channel  $i$ , then

$$\rho_i = \sum_{\lambda} C_{i\lambda}, \quad (3)$$

where  $C_{i\lambda}$  is the total number of counts in channel  $i$  due to the  $\lambda$ th element. The pulse height spectra of the monoelemental components can be normalized as follows:

$$C_{i\lambda} = \beta_{\lambda} A_{i\lambda}, \quad (4)$$





where  $A_{i\lambda}$  is the normalized number of counts in channel  $i$  due to the element  $\lambda$ , and  $\beta_\lambda$  is the relative intensity of the  $\lambda$  component, then

$$\rho_i = \sum_{\lambda} \beta_{\lambda} A_{i\lambda} \quad (3a)$$

Another component of the measured pulse height spectra which must be considered is the background. In the case of alpha induced fluorescence there are two separate sources of radiation contributing to the background spectrum (see Figures 3 and 6). As indicated above, one component can be attributed to the natural background and to gamma rays from the source striking the detector. The second component can be attributed to the x-rays emanating from the source being scattered by the sample. We have found that in this instance the major contribution to the background seems to be due to this second scattered component. The amount of scatter will depend on the average atomic number of the sample and thus changes from sample to sample. We have found further from our measurements that while the shape of the background pulse height spectrum does not change significantly from sample to sample the intensity does. Further study of the shape of the background as a function of composition is underway. The problem of subtracting background is not a simple one. Our approach to this problem will be described in detail, in the final section of this paper where actual spectral analyses will be presented. Figure 6 shows the measured pulse height spectrum of a basalt sample with the background included. Equation (3a) should include the background component  $B_i$ , where  $B_i$  (see Figure 3) is the intensity of the background in channel  $i$ :

$$\rho'_i = \sum_{\lambda} \beta_{\lambda} A_{i\lambda} + B_i. \quad (3b)$$

### C. Formulation of the Linear Least Square Analysis

1. Matrix Equations: If equation (3b) were truly an equality the relative intensities  $\beta_\lambda$  could easily be determined by a simple matrix inversion of (3b) that is

$$\vec{\beta} = (A^{-1}) \vec{\rho}, \quad (4)$$

where  $\beta$  is a vector of the relative intensities,

A is a  $m + n$  matrix of the monoelemental components, and

$\rho$  is a vector of the measured polyelemental spectrum minus background  $(\rho'_i - B_i)$ .

The problem in performing this inversion arises when one considers the statistical variance in the measurement  $A_{i\lambda}$ , and  $\rho_i$ . Because of this, the equality (3b) is not true and a unique solution to (4) does not exist. Equation (4) is overdetermined, therefore an infinite set of equally good solutions is possible and there are no criteria for selecting the best one. As a consequence of this and because of the statistical variance involved only the most probable values of  $\beta_\lambda$  can be determined by using the following criterion.

$$M = \sum_i \omega_i (\rho'_i - \sum_\lambda \beta_\lambda A_{i\lambda})^2 \rightarrow \text{minimum}, \quad (5)$$

where  $\omega_i$  is a statistical weighting function and is proportion to  $1/\sigma_i^2$ , and  $\sigma_i^2$  is the statistical variance in the measurement in channel  $i$ .

In formulating the linear least square analysis method we begin by assuming that the pulse height scale is invariant (i.e., there is no gain shift or zero drift) and, therefore, the minimum can be found by taking a partial derivative with respect to some relative intensity  $\beta_\gamma$ . The derivative is then set equal to zero:

$$\frac{\partial M}{\partial \beta_y} = \sum_i \omega_i (\rho_i - \sum_{\lambda} \beta_{\lambda} A_{i\lambda}) A_{iy} = 0 \quad (6)$$

This can be written in matrix form as a no longer overdetermined set of equations

$$\tilde{A}\omega\rho - (\tilde{A}\omega A) \beta = 0, \quad (6a)$$

where the definition given in (4) still holds and

$\omega$  is a diagonal matrix of the weighting function  $\omega_i$ , and

$\tilde{A}$  is the transpose of the  $A$  matrix. Solving for the relative intensity vector  $\beta$ , we find that

$$\beta = (\tilde{A}\omega A)^{-1} \tilde{A}\omega\rho \quad (6b)$$

where  $(\tilde{A}\omega A)^{-1}$  is the inverse matrix of  $(\tilde{A}\omega A)$ . Essentially it is the method of attaining the solution of equation (6b) which will concern us in the rest of the discussion. This equation has been applied to the solution of a number of spectroscopic problems involving pulse height analyses<sup>12, 13, 14, 15, 16, 17, 18</sup>. There are a number of questions which must be answered in determining the algorithm (i.e., the method of solution) to be used for the given problem:

1. Is it possible to invert the matrix  $(\tilde{A}\omega A)$ ?
2. Are the components of the  $A$  matrix linearly independent or do they correlate?
3. How does one calculate this effect?
4. How does resolution effect the correlation?
5. What is the nature of the  $\omega$  matrix?

6. What is the effect of background subtraction?

7. Is the system linear?

8. If there are non-linearities in the system, how does one compensate for non-linearities in the application of this method?

2. Library Functions: Let us consider the X-ray emission method, and determine the algorithm for obtaining  $\beta$  from equation (6b). We start by considering the nature of the A matrix. The rows of the matrix can consist of either the monoelemental pulse height spectra (i.e., spectra characteristic of all the possible elements found in the irradiated sample) or the monoenergetic pulse height spectra (i.e., the pulse height spectra characteristic of all the possible monoenergetic x-rays striking the detector). Since we are interested in qualitative and quantitative elemental composition, we will consider the problem using the monoelemental pulse height spectra.

The monoelemental pulse height spectra are determined by irradiating pure samples of the elements in the same geometric configuration as that used for the unknowns. Because these measurements have an inherent statistical error and because of the dynamics of the measurement system (possible gain drifts and zero drifts), these monoelemental pulse height spectra can be determined to only two or perhaps three significant figures with any great certainty. In the solution proposed in this paper, the statistical errors in the measurement of the monoelemental pulse height spectra are kept much smaller than the error in the measurement of the unknown pulse height spectra by extended and repeated measurements and therefore can be ignored. The difficulty comes then when an attempt is made to invert  $(\bar{A}\omega A)$ . This inversion requires obtaining differences involving the third, fourth, and even fifth significant figure. As indicated above

the measurements of the monoelemental spectra are only good to two and at the most three significant figures. Thus, unless some additional constraints are introduced serious oscillations in the solution will result, and in fact one cannot successfully invert the matrix. Two necessary constraints that can be imposed are symmetry conditions of the  $(\tilde{A}\omega A)$  matrix and also a "non negativity option." The symmetry constraint follows from matrix algebra and is accomplished in the program which examines the symmetric off diagonal elements, i.e., the  $A_{ij}$  and  $A_{ji}$  where  $i \neq j$  and sets them equal. The use of the non negativity option which proves very useful to the x-ray case will be further amplified.

3. Non-negativity Constraint: It has been shown above that an exact solution cannot be obtained because of the statistical variation in the measurement. If such exact solutions were possible, the relative intensity of the various components would either be positive or zero. Now we are looking for the most probable solution, and in this case negative values can appear. When such negative values are observed, there must be an associated error which is as great or greater than the absolute magnitude of the value obtained. Negative values with errors significantly smaller than the absolute value do however appear in the application of least square analysis to the reduction of pulse height spectra. It is this effect which produces oscillations in the solution described above.

The oscillation in the solution can be described in the following way. A given relative intensity can appear as a negative value, and possibly more negative than it should be because of the errors in the inverse transformation just discussed. The overestimation of a negative component by the analytical method will tend to make some other component more positive to compensate. This in turn will tend to make a third component smaller than it should be in

order to compensate, and thus an oscillation in the solutions will be produced. By imposing a non-negativity constraint one essentially damps out these oscillations in the solution due to such factors as errors in the determination of the A matrix, and errors in improperly subtracting the background. What is meant by the non-negativity constraint then, is that when determining the relative intensities of the  $\beta$  vector (6b), only positive values of monoelemental components are allowed, and negative values are set equal to zero.

The use of physical constraints in the solution of linear least square analyses was first discussed by Beale<sup>19</sup>, and suggested for use in the analysis of pulse height spectra by Burrus<sup>13</sup>. A method using the non-negativity constraint for the analysis of gamma ray pulse height spectra<sup>12, 13</sup> is now being applied to the problem of x-ray non-dispersive analyses and has been discussed briefly in other papers<sup>1, 4</sup>.

Because of the necessarily empirical nature of the method of solution the absolute minimum obtained from equation (6b) is not necessarily the best solution. One must find a minimum in the domain described by other physical constraints. In addition to non-negativity, one should consider the following constraints, for example:

1. If the relative intensities of two species be known, then the ratio of intensities is invariant in the least square analysis.
2. The sum of the relative intensities once determined for various elements always equals some constant.

Later in the discussion concerning limits of resolution and correlation the latter condition will be invoked to help in the solution. Continuing with the discussion of a non-negativity constraint, we shall give only a brief and

non-rigorous physical argument to show how one obtains a solution (since a detailed description of this solution is given elsewhere<sup>12, 13, 19</sup>). We first assume that we have a linearly independent set of monoelemental functions (function library  $A_{ij}$ ) and we are required to find the relative intensities ( $\beta_\lambda$ ) of these library functions which combined will yield the best fit to the experimentally determined polyelemental pulse height spectrum (raw data spectrum  $\rho$ ). The library must include all possible components. We now assume that all but two components from the library are zero. A least square fit (6b) to the total spectrum  $\rho$  is used to determine the relative intensity of these two components. Since the number of components in the measured spectrum  $\rho$  is generally equal or larger than two, the estimates of the relative intensities of these two components will be greater than they should be. As components from the library are added, the relative intensities of the individual components will grow smaller. Thus if the least square fit gives a negative relative intensity for either of these two components, that component is eliminated from the library of elements and not used in the analyses (i.e., its relative intensity is set equal to zero). If both relative intensities are positive, both components are kept. Additional library components are added, one at a time, at least a square fit is made, and all negative components are again set equal to zero. The process is continued until all components have been tested. This then will yield the desired solution which is the least square solution for relative intensities in the positive domain. If the library elements are linearly independent then the solution obtained will be completely independent of the order in which the mono-elemental components are added.



The question may be asked concerning the necessity to perform the iterative process described above in order to find the solution to the minimum in the positive domain. Why not, for example, find the absolute minimum with all the components at once and then adjust the negative values to zero. The answer is that because of the possibility of oscillation in the solution, it is difficult to tell whether the negative values result from the oscillations in the solution or because of true statistical variation. The non-negativity, as we have indicated, tends to damp this oscillation out, and the algorithm described above finds the desired solution.

One must be rather careful in using this non-negativity principal for strictly speaking, negative solutions should be allowed in least square analysis. What the non-negativity constraint does is to increase the mathematical error because one does not find the absolute minimum as required by the least square method. Furthermore, by rejecting certain components, estimates of possible minimum detectable limits for these components are not determined. In order to obtain the minimum detectable limits in the program prepared for this analysis, both the absolute minimum and the minimum in the positive domain can be found, and compared.

4. Error Calculation: We now consider the problems of calculating the error in the relative intensity  $\beta_\lambda$  due to the statistical variation in  $\rho_i$ , the counts in channel  $i$ , contributed by the components of the polyelemental pulse height spectrum. Let us consider equation (6b), which shows that  $\beta_\lambda$  can be written as a linear combination of the  $\rho_i$ 's:

$$\beta_\lambda = \sum_i \sum_\nu C_{i\lambda}^{-1} A_{i\nu} \omega_i \rho_i \quad (6c)$$

We define  $C = (\tilde{A}\omega A)$ , where  $(\tilde{A}\omega A)$  is a symmetric matrix whose elements  $C_{\nu\gamma}$  of  $C$  are given by

$$C_{\nu\gamma} = \sum_i \omega_i A_{i\nu} A_{i\gamma}$$

Remembering that  $\omega_i$  is the statistical weight and  $\omega_i = 1/\sigma_i^2$  where  $\sigma_i^2$  is the variance of the measurement of  $\rho_i$  in channel  $i$ , and  $C^{-1}$  is the inverse of matrix  $C$ , e.g.,

$$CC^{-1} = I, \quad (9)$$

and where  $I$  is the identity matrix (i.e., all off diagonal elements are zero and the diagonal elements are one) or

$$\begin{aligned} I_{\nu\lambda} &= 1 \text{ if } \nu = \lambda \\ I_{\nu\lambda} &= 0 \text{ if } \nu \neq \lambda \end{aligned} \quad (10)$$

The elements of the  $I_{\nu\lambda}$  can be given

$$I_{\nu\lambda} = \sum_{\gamma} C_{\nu\gamma} C_{\gamma\lambda}^{-1} \quad (11)$$

From equation (6c), it is seen that  $\beta_\lambda$  is a linear homogeneous function of the counts  $\rho_i$  under the assumption that there is no significant error in the  $A_{ij}$  compared to the measurement of  $\rho_i$ . Thus the mean square deviation  $\sigma^2(\beta_\lambda)$  corresponding to the variation in  $\rho_i$  can be written as a linear sum of the variances on the  $\rho_i$ 's. Thus from equation (6c) we get the variance for  $\beta$  to be

$$\sigma^2(\beta_\lambda) = \sum_i \sum_{\nu} \sum_{\gamma} C_{\nu\lambda}^{-1} C_{\gamma\lambda}^{-1} A_{i\nu} A_{i\gamma} \omega_i^2 \sigma^2(\rho_i), \quad (12)$$

and from (8),

$$\sigma^2(\beta_\lambda) = \sum_i \sum_\nu \sum_\lambda C_{\nu\lambda}^{-1} C_{\gamma\lambda}^{-1} A_{i_\nu} A_{i_\gamma} \omega_i$$

or

$$= \sum_\nu \sum_\lambda C_{\nu\lambda}^{-1} C_{\gamma\lambda}^{-1} \sum_i \omega_i A_{i_\nu} A_{i_\gamma}$$

Then from (7),

$$\sigma^2(\beta_\lambda) = \sum_\nu \sum_\gamma C_{\nu\lambda}^{-1} C_{\gamma\lambda}^{-1} C_{\nu\gamma}$$

or

$$\sigma^2(\beta_\lambda) = \sum_\nu C_{\nu\lambda}^{-1} \sum_\gamma C_{\nu\gamma} C_{\gamma\lambda}^{-1}$$

and from equation (11)

$$\sigma^2(\beta_\lambda) = \sum_\nu C_{\nu\lambda}^{-1} I_{\nu\lambda}.$$

Finally from (10)

$$\sigma^2(\beta_\lambda) = C_{\lambda\lambda}^{-1}, \quad (13)$$

that is,  $\sigma^2(\beta_\lambda)$  can be found from the diagonal elements of the  $C^{-1}$  matrix.

Equation (13) is true if  $\chi_i^2$  is equal to one.  $\chi_i^2$  is defined as follows:

$$\chi_i^2 = \frac{\sum_i \omega_i (\rho_i - \sum_\lambda \beta_\lambda A_{i\lambda})^2}{n - m} \quad (12)$$

where  $n-m$  are the number of degrees of freedom,

$n$  is the number of channels, and

$m$  is the number of library components.

If  $\chi_i^2 \neq 1$ , then

$$\sigma^2(\beta_\lambda) = \chi_i^2 C_{\lambda\lambda}^{-1}. \quad (13a)$$

$\chi_i^2$  and its utilization will be discussed in slightly more detail below.

5. Correlation: Let us now consider what we mean by linearly independent library functions. It was shown that  $C_{\lambda\lambda}^{-1}$  is the variance on  $\beta_\lambda$ . It can be further shown that  $C_{\lambda\gamma}^{-1}$  is the covariance of  $\lambda'$ th and  $\gamma'$ th component<sup>20,21</sup>. A measure of interferences  $F_{\lambda\gamma}$  between the  $\lambda'$ th and  $\gamma'$ th component is given by

$$F_{\gamma\lambda} = \frac{(C_{\gamma\lambda}^{-1})^2}{(C_{\lambda\lambda}^{-1})(C_{\gamma\gamma}^{-1})} \times 100\% \quad (14)$$

Equation (14) is a measure of how different, or how well one component or library spectrum can be resolved from another. It is also a measure of whether or not the components in the library of spectra can be considered to be linearly independent.

As an illustration of how equation (14) is used, let us assume that the library function or monoenergetic functions can be described by Gaussians:

$$A_{i\lambda} = \exp - \frac{(i - P_\lambda)^2}{2\alpha_\lambda^2}, \quad (15)$$

where  $A_{i\lambda}$  is the normalized counts in channel  $i$  due to the  $\lambda'$ th component,

$\alpha_\lambda^2$  is a constant and is a measure of the width of the Gaussian for energy  $\lambda$ ,

and  $P_\lambda$  was defined in equation (1).

Now let us calculate the percent inference between two monoenergetic pulse height spectra with Gaussian form using equation (14) and a shape given by (15).

If we assume no statistical error, equation (14) can be written

$$F_{\gamma\lambda} = \frac{\sum_i A_{i\gamma} A_{i\lambda}}{\left(\sum_i A_{i\gamma}\right)^2 \left(\sum_i A_{i\lambda}\right)^2} \quad (14a)$$

Using equations of the form given in (15) for  $A_{i\gamma}$  and  $A_{i\lambda}$  and replacing the summation by an integral from - infinity to + infinity (14a) becomes

$$F_{\gamma\lambda} = \frac{\int_{-\infty}^{+\infty} \left[ \exp - \frac{(i - P_\gamma)^2}{2\alpha_\gamma^2} \exp - \frac{(i - P_\lambda)^2}{2\alpha_\lambda^2} \right] di}{\left[ \int_{-\infty}^{+\infty} (di) \exp - \frac{(i - P_\gamma)^2}{2\alpha_\gamma^2} \right]^2 \left[ \int_{-\infty}^{+\infty} \exp - \frac{(i - P_\lambda)^2}{2\alpha_\lambda^2} (di) \right]^2} \quad (14b)$$

$$= \frac{2\alpha_\lambda \alpha_\gamma}{\alpha_\lambda^2 + \alpha_\gamma^2} \exp - \frac{P_\lambda - P_\gamma}{-\alpha_\lambda^2 + \alpha_\gamma^2}$$

The constant  $\alpha_\gamma$  can be written in terms of the resolution  $R_\gamma$  as

$$\alpha_\gamma = \frac{R_\gamma P_\lambda}{2 \sqrt{2 \ln 2}} \quad (16)$$

Remember that  $P_\gamma$  stands for the pulse height portion of some energy  $E_\gamma$  and is proportional to  $E_\gamma$ . If we now assume that equation (2) is applicable and let  $n = .5$ , we get

$$\frac{R_\gamma}{R_\lambda} = \sqrt{\frac{P_\lambda}{P_\gamma}} \quad (17)$$

For this special case we can substitute equation (17) into equation (14b)

$$F_{\gamma\lambda} = \frac{2 \sqrt{P_\lambda P_\gamma}}{P_\lambda + P_\gamma} \exp - \frac{P_\gamma (P_\lambda - P_\gamma)^2}{(P_\lambda - P_\gamma) \alpha_\lambda^2} \quad (14c)$$

Figure 7 is a plot of Equation (14c) for various detector resolutions as a function of the percent separation  $(P_\gamma - P_\lambda)/P_\lambda$  for decreasing  $P_\gamma$ , where  $P_\gamma$  and  $P_\lambda$  are the axis for two adjacent energies. If  $P_\gamma = P_\lambda$ , the Gaussians are identical and the percent interference is 100%. As  $(P_\gamma - P_\lambda)$  increases the percent interference decreases, and this is then a measure of how well the two Gaussians can be resolved. For example, consider the following case. Given

1. Two x-ray energies separated by 10%,
2. The detector resolution for the higher energy is 20%,
3. The relationship given in equation (17) holds, and
4. The photopeak is described by a Gaussian which fully described the pulse height spectrum of the monoenergetic component (e.g., no escape peak or continuum), there will be a 50% interference between these energies.

The sum  $\beta_\gamma + \beta_\lambda$  can be determined and will be constant, but both  $\beta_\gamma$  and  $\beta_\lambda$  can be varied by 50% keeping their sum constant and the fit based on the least square criteria will be just as good. In general given a library of functions  $A$ , the percent interference between various components can be determined by forming  $(\bar{A}A)^{-1}$  and calculating  $F_{\gamma\lambda}$  from (14). This point will be described further in Section III, where a solution of an actual experimental problem is presented.

If two functions do interfere strongly, it is sometimes possible to impose a physical constraint, which can eliminate the interference. For instance, in the problem of gamma ray spectroscopy with a mixture of isotopes with varying half lives, the pulse height spectra can be followed until one of the species has decayed out. The second specie is then followed and the intensity determined. Knowing the half life of the second species, the intensity of the second component

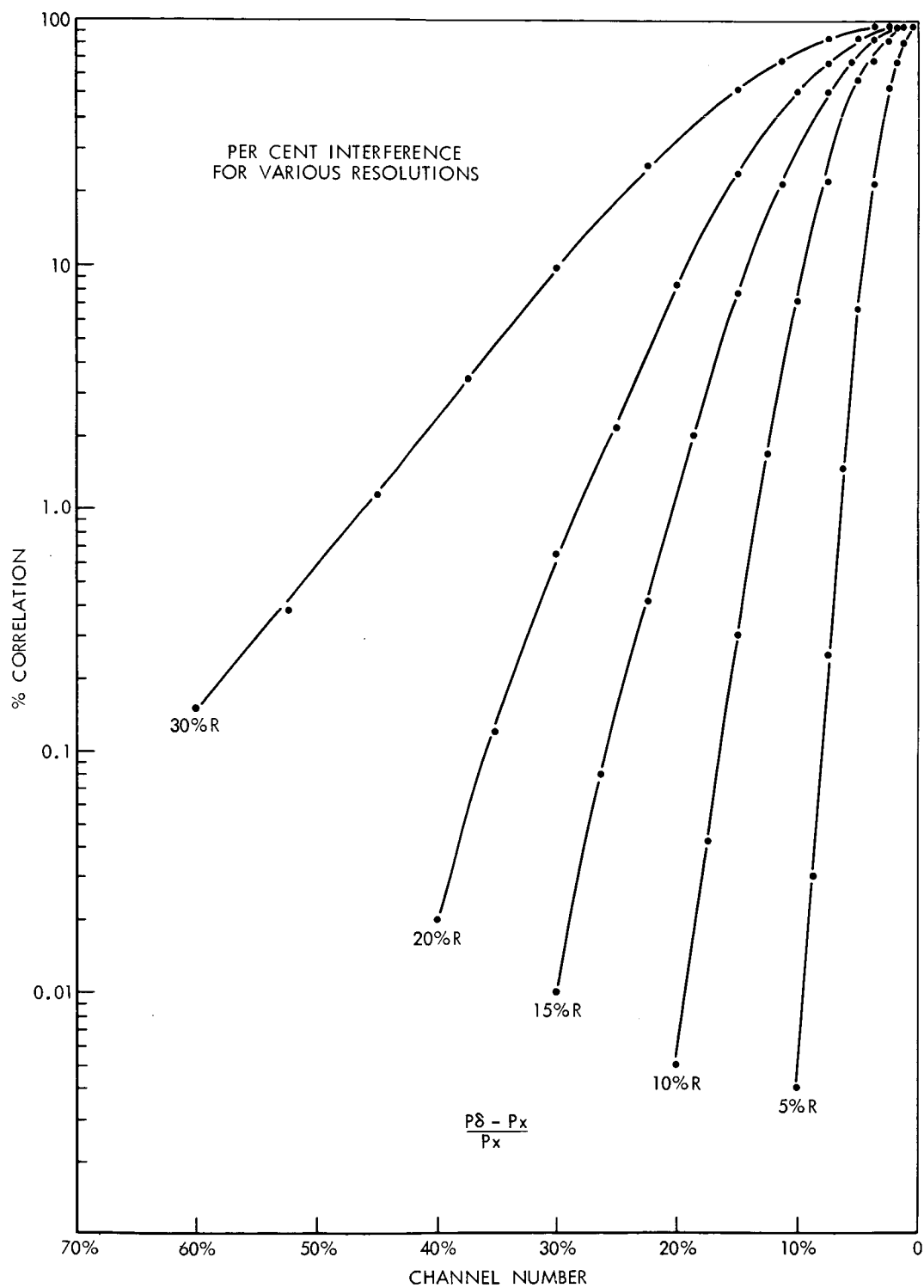


Figure 7

can be determined and extrapolated back to the earlier measurements when the correlation was large. The second component can then be stripped out and the analysis repeated for the first element with the correlation due to the second element eliminated. In x-ray fluorescence, on the other hand, it is possible to use filters, and determine either the intensity of one energy or determine the ratio of one energy with respect to another. Using the intensity of one component or the ratio of one component to another as a physical constraint, the interference can be eliminated.

The percent interference described above has only considered the problem of resolution, but there are two other effects which will produce strong interference. In one case the statistical error due to counting and background subtraction may be so high that the percent interference will be large. This will be related to the statistical weight  $\omega$  in the  $(A\omega A)^{-1}$  equation. Secondly, interference can occur between two elements if the library is incomplete and an element is missing. Then the two components on either side of the missing element will be under or overestimated in order to make up for the missing element and the two adjacent elements will correlate. When one calculates the difference between the measured spectrum and the calculated spectrum using least squares, a negative or positive peak will appear at the position of the missing element. By adding in the missing component, the interference and  $\chi^2_i$  can be greatly reduced.

6. Chi Square: In the method developed for this problem a  $\chi^2_i$  test is performed (see Equation 12) for goodness of fit. The closer  $\chi^2_i$  is to unity the better the fit.

7. Background Correction: At first thought, this problem should be rather simple to handle. For example, a background is measured for either the same



time or a time longer than the measurement of the unknown system, and then the background is subtracted with adjustment being made for the counting times. In x-ray fluorescence a major part of the background is due to coherent scattering from the sample of the incident radiation. Thus, the fraction of background to be subtracted will be affected by the nature of the sample (average atomic number, density, etc.). However, as an alternative approach the following method was used. Measurements of the raw data spectrum  $\rho$  are made to extend to energies (or pulse height channels) higher than the highest energy expected in the pulse height spectrum due to the sample. A background spectrum using a strong scatterer such as boric acid or plastic in the sample position is taken. Characteristic x-rays from these substances are so soft as to remain undetected by our present instrumentation. As was pointed out in the section on the shape of the pulse height spectra, the shape of the background spectrum does not seem to be strongly affected by the scatterer although the intensity is greatly affected. The background is then included as a library component and subjected to the least square treatment, already described, which yields a measure of the background intensity included in the total spectrum. In practice this latter approach has proven feasible because in the measurement of the raw data spectrum  $\rho$  there is a higher energy portion of the background spectrum which is free of lines generated in the specimen. If this were not the case, the background spectrum would strongly correlate with each of the monoelemental components, and a unique solution would not be obtained. In this event one goes back to the subtraction technique. This second approach has also been used, but since an iterative process is necessary, it is more time consuming. This follows because the fraction of background to be subtracted is not known and can only be arrived

at by trial and error, e.g., various fractions are subtracted, subjected to least square analysis and a minimum  $\chi_i^2$  sought. In this study, the results presented in the paper used the method of including the background as a library component although the computer program developed has the subtract option included. Included as part of this second option is an error calculation due to this subtract mode and a proper evaluation of the weighting function  $\omega$  used in the least square analysis.

8. Gain Shift: Up to this point it has been assumed that the pulse height scale for the library spectra is the same as that for the measured raw data spectrum  $\rho$ . Because of the possibility of gain shifts, and zero drift, the pulse height scale can be compressed or expanded and linearly shifted. Two approaches can be used to compensate for this effect. Non-linear least square analysis methods may be used. That is, in equation (5), the derivative with respect to  $\beta_\gamma$  and  $A_{i\gamma}$  can be obtained. This technique is rather complex, but a number of methods have been developed<sup>22, 23</sup>. Because of these complexities we have used the linear method, and make corrections to the raw data vector  $\rho_i$  before performing the analysis. Other similar techniques have been developed<sup>13, 15, 18, 24</sup>.

Let us first consider the problem of gain shift. It must be remembered that the measured pulse height spectrum is a histogram, that is, it is a measure of all pulses in some increment  $\Delta i$  about  $i$  as a function of  $i$ . The total sum  $\sum_i \rho_i$  is equal to the total number of interactions between the incident x-ray flux and detector. This number must remain a constant for a given measurement and is independent of a compression, extension, or linear translation along the pulse height axis. If we assume that there is a gain shift  $G$  on the pulse height axis between library spectra  $A_{ij}$  and the raw data spectrum  $\rho$ , the pulse scale  $i$

will have to be multiplied by  $G$  and the count rate scale  $\rho_i$  divided by  $G$  to compensate for the shift. This keeps the area a constant.

It is important to point out that the library spectra histograms are only included for integer values of pulse height which are separated by  $\Delta i = 1$ . The gain is shifted by some value  $G$  which will produce values at fractional pulse heights and cause  $\Delta i$  to become either greater or less than unity. For example consider the case for  $G = .98$  or  $G = 2.0$ . Channels ten and eleven will become channels 9.8 and 10.78 for  $G = .98$  and channels 20 and 22 for  $G = 2.0$ . For the first case  $G = .98$ , we must find the value at channel 10, 11, 12, etc. and for the second  $G = 2.0$  we would have to find the value at channel 20, 21, 22, etc. The value at channel 10 ( $G = .98$ ) or at channel 21 ( $G = 2.0$ ) is found in our method by linear extrapolation which is an integral part of our program. Only two points are used at a time in this extrapolation. Higher order methods can also be used, but have not been found necessary in this application.

Two choices are possible: shifting the library spectra to correspond to the raw spectrum or visa versa. The second alternative has been found more economical in terms of time. The results obtained using either alternative are the same.

In practice either a given gain shift or a range in gain shift ( $G_{\min}$  and  $G_{\max}$ ) is assumed. A series of least square fits between the assumed  $G_{\min}$  and  $G_{\max}$  are made,  $\chi_i^2$  calculated and the minimum  $\chi_i^2$  found for this range. Figure 8 shows a measured spectrum and the gain shifted spectrum. The spectrum has been shifted 30%.

A similar method compensating for zero drift is now being developed for inclusion in the program. Here a minimum  $\epsilon_{\min}$  and maximum  $\epsilon_{\max}$  is

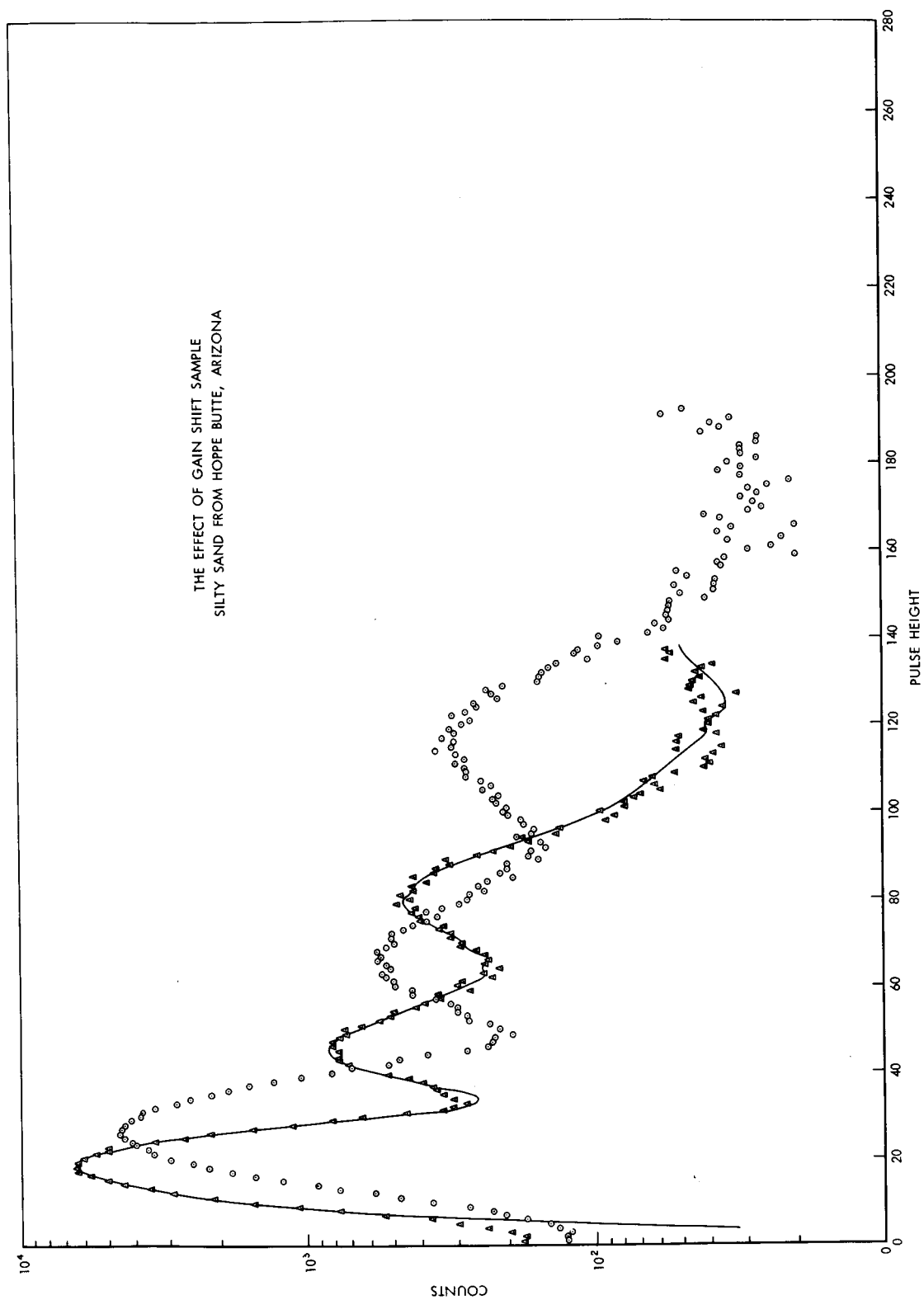


Figure 8

introduced. The pulse height scale is shifted by a value  $\epsilon$ , the intercepts at integer pulse height values are then determined, and again least square fits are made until a minimum  $\chi_i^2$  is determined in the range  $\epsilon_{\min}$  to  $\epsilon_{\max}$ .

9. Computer Program: The computer program flow diagram which has been developed to perform the above described calculations is shown in Figure 9. The zero shift part of the program is not included in the flow diagram. There are four flows available in this program. Flow 1 allows the stripping of one or more components from the spectrum before analysis. Flow 2 allows background subtraction, gain shifting of the spectrum, and contains the non-negative constraint as an option. Flow 3 is just a flow for solving equation (5) without gain shift and without subtraction of background, and without the non-negativity constraint. Flow 4 is similar to Flow 2, but does not allow for background subtraction. Calculation for errors introduced due to stripping of components and background subtraction are included in the appropriate flow. A number of options are allowed for calculation of  $\omega \cdot \omega$ , the statistical weight matrix, can be either (1) set equal to the unity matrix, (2) set equal to  $1/\rho$ , (3) calculated internally in Flows 1, 2 and 4, or (4) read in separately according to the analysts desire. The output from the computer program yields the following information: (1) the flow used, (2) the gain for minimum  $\chi_i^2$  if the option is chosen, (3) whether or not the non-negativity constraint was used, (4) the relative intensities for  $\beta$ , (5) the mono-elemental library functions used, (6) the elements rejected if non-negativity is used, (7) the standard deviation corresponding to each of the relative intensities calculated, (8) the percent interference between library elements, (9) the actual spectrum analyzed, (10) the synthesized spectrum obtained using the relative intensities determined by least square, (11) the difference between the actual and

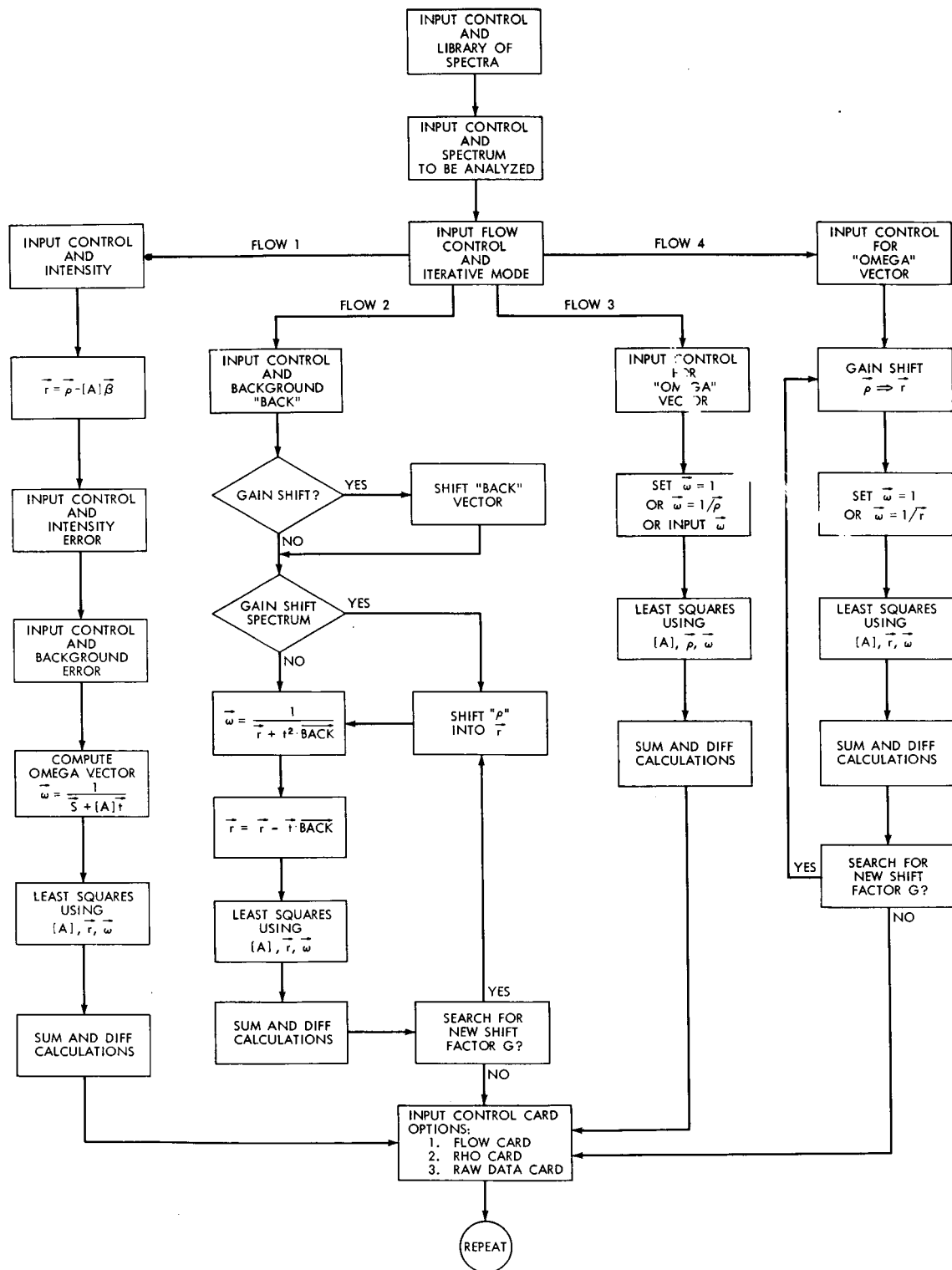


Figure 9

synthesized spectrum, (12) and the  $\chi^2_i$  value. A more detailed description of the program can be found in references<sup>10,11,22</sup>.

### III. APPLICATION OF LEAST SQUARE TECHNIQUE TO AN EXPERIMENTAL PROBLEM

#### A. General Experimental Results

The procedures which have been described in some detail above have been applied to the problem of the semi-quantitative determination of the composition of a variety of rock types ranging from ultra-basic rocks such as dunite and peridotite through acidic rocks such as granite. For this purpose a suite of six rocks, carefully prepared by the U. S. Geological Survey and presently being circulated for comparative analysis were used. All rock samples were finely divided and homogenized.

Library spectra were obtained using oxides and carbonates of the various elements to be determined such as Mg, Al, Si, K, Ca, Ti, Mn and Fe.

For the measurements reported here, a sealed A-CH<sub>4</sub> proportional counter was used which gave a resolution of 17.5 percent of the Mn K $\alpha$  line from Fe<sup>55</sup>.

Background was determined using a boric acid briquet as a scatterer. Figures 10-15 show the observed spectra for dunite, peridotite, basalt, andesite, granodiorite and granite. These experimentally measured data are shown as points superimposed on the solid line curves, synthesized by the computer using the least square technique proposed and the library elements.

In every instance the spectra have been gain shifted so that they are on a common pulse height energy scale. On this basis one can state that up to approximately channel 90, covering the elemental range from Mg to Fe, the agreements are excellent and in fact within the statistical error. Beyond channel 90

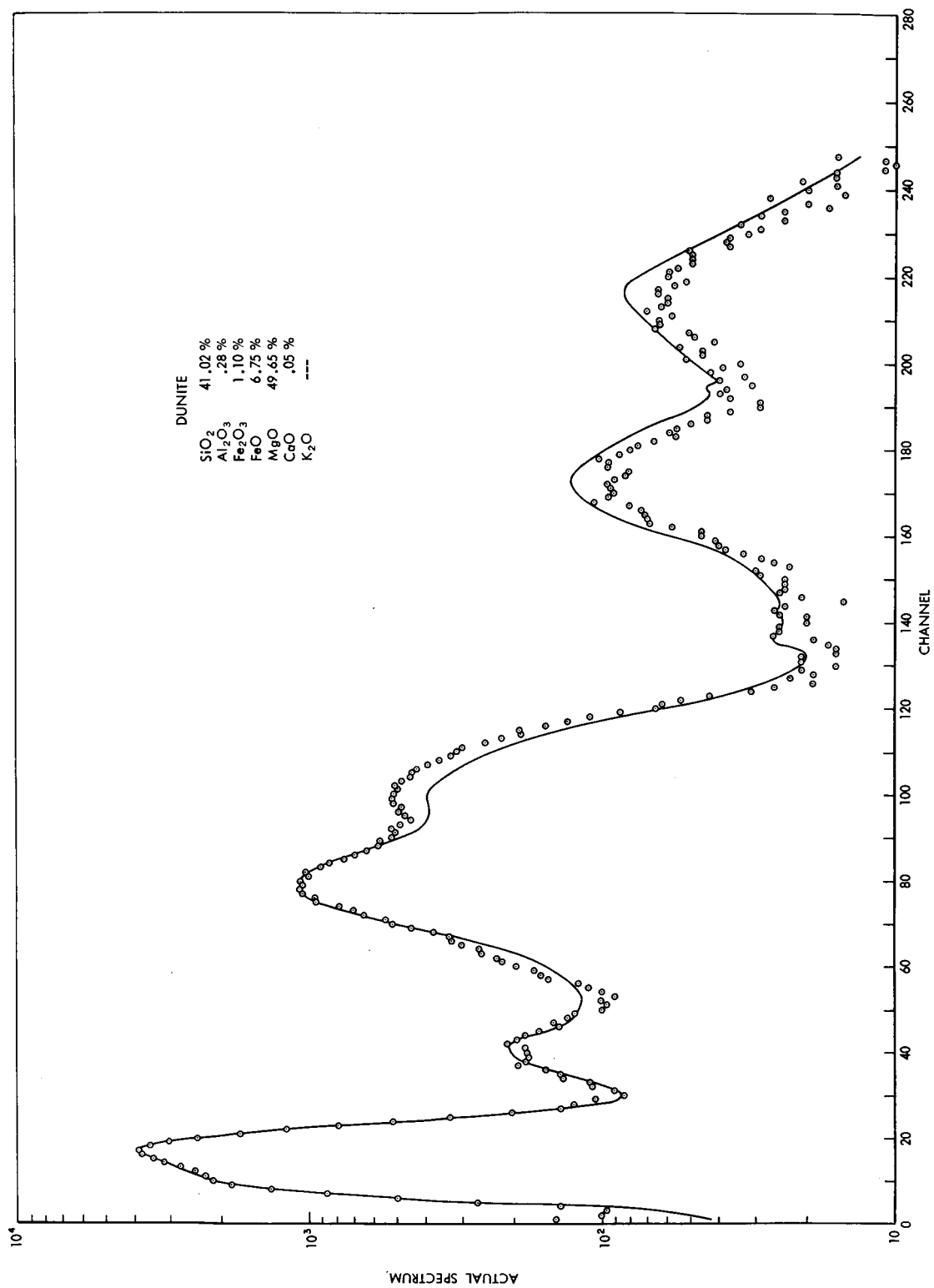


Figure 10



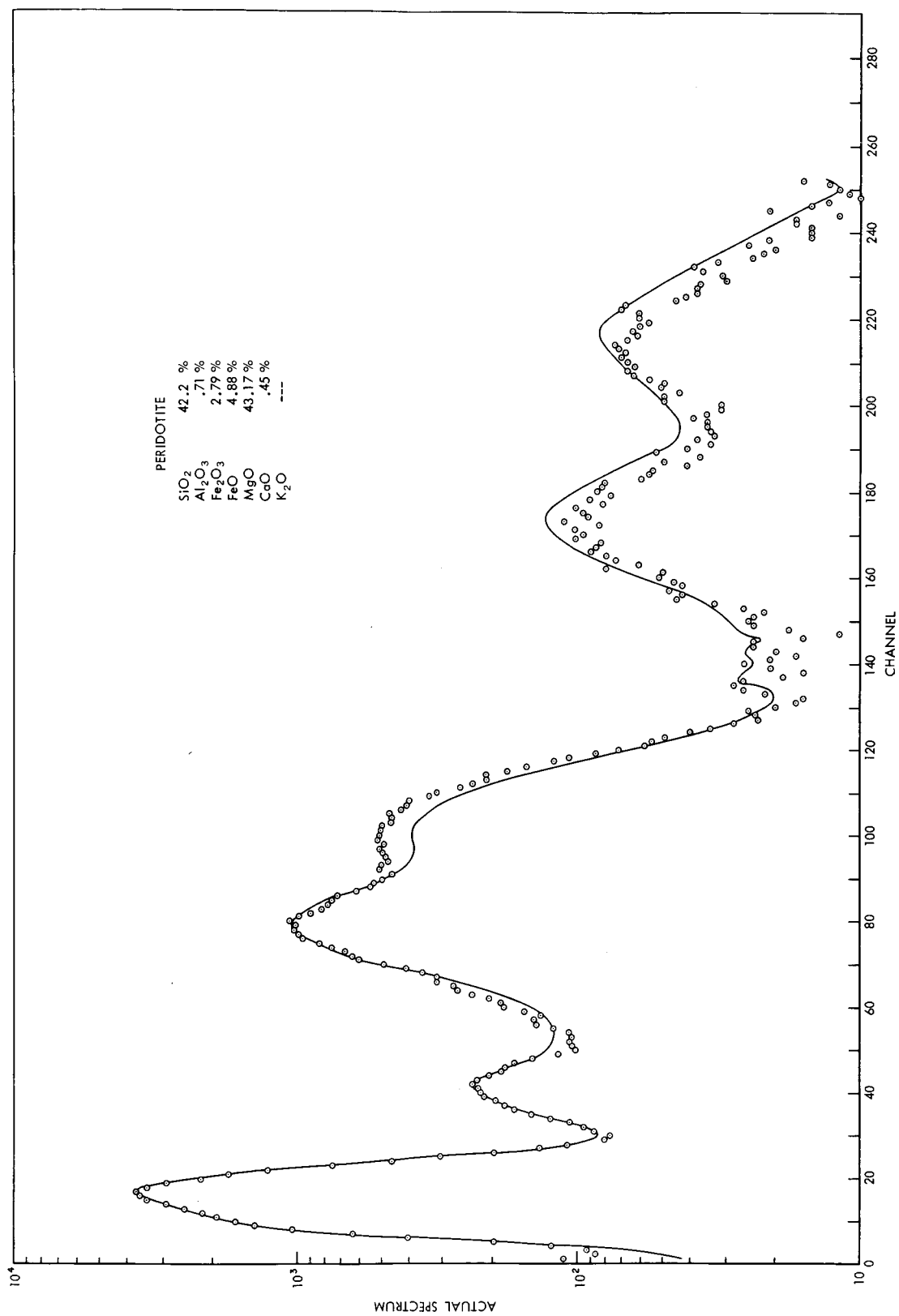


Figure 11

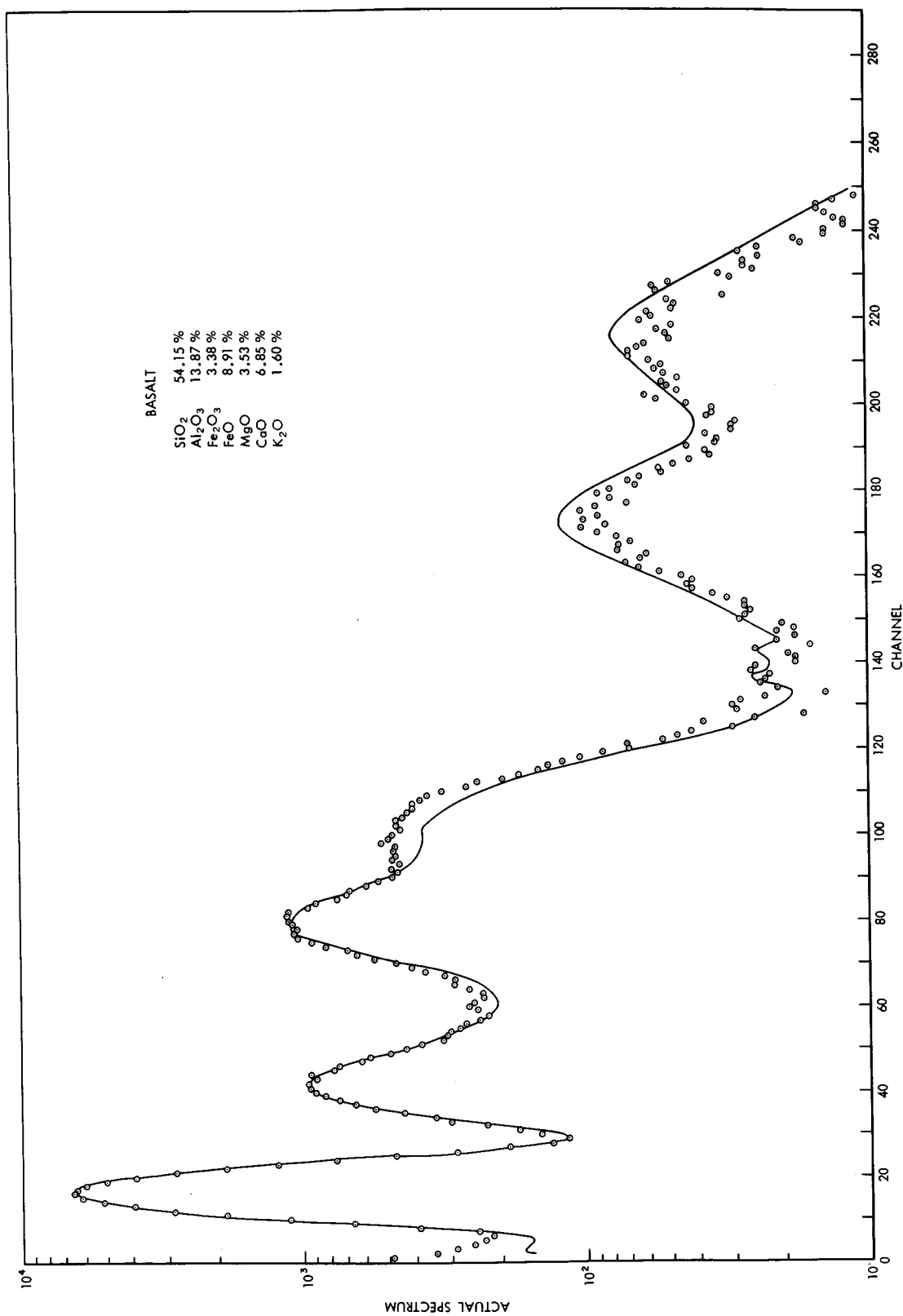


Figure 12

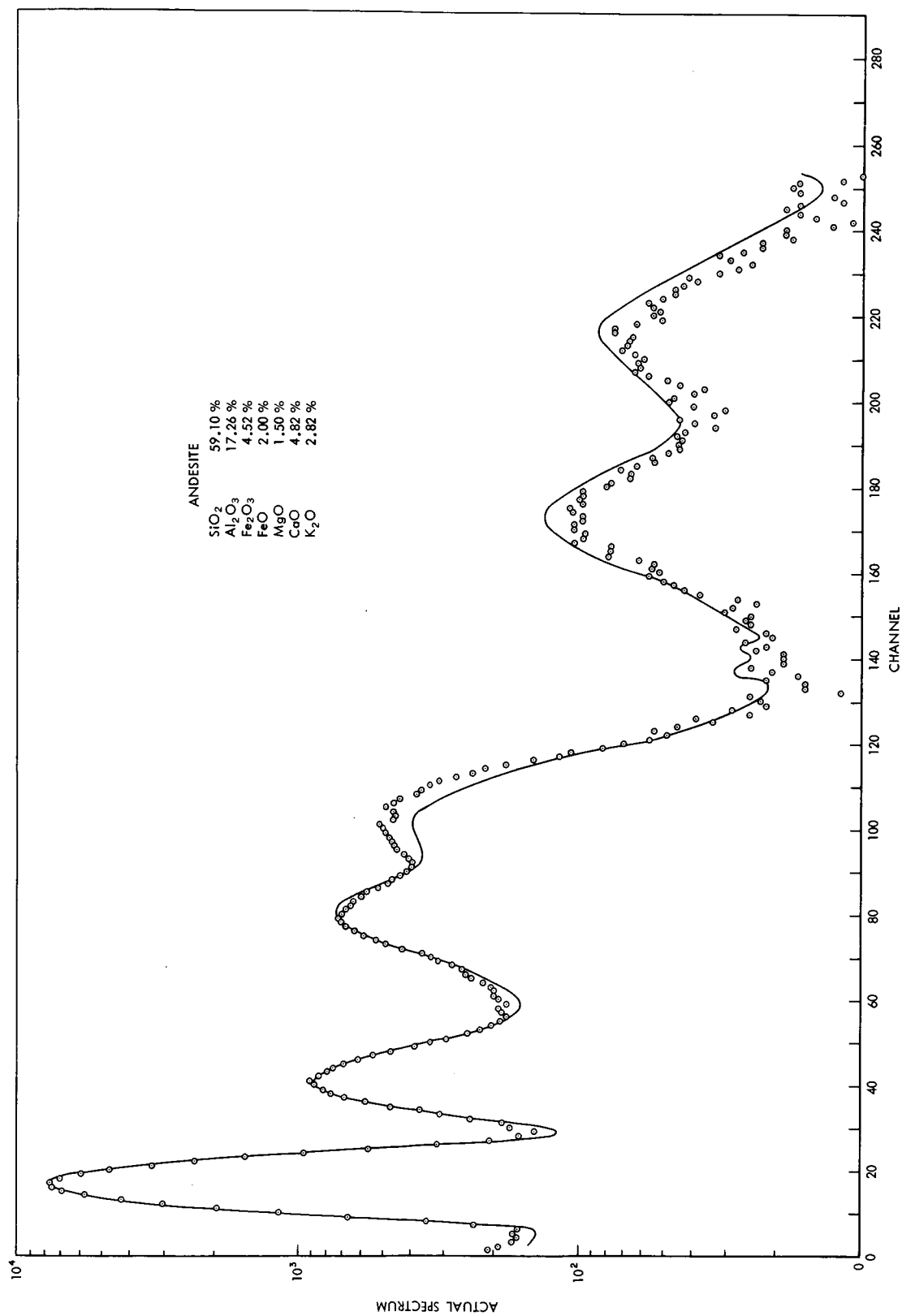


Figure 13

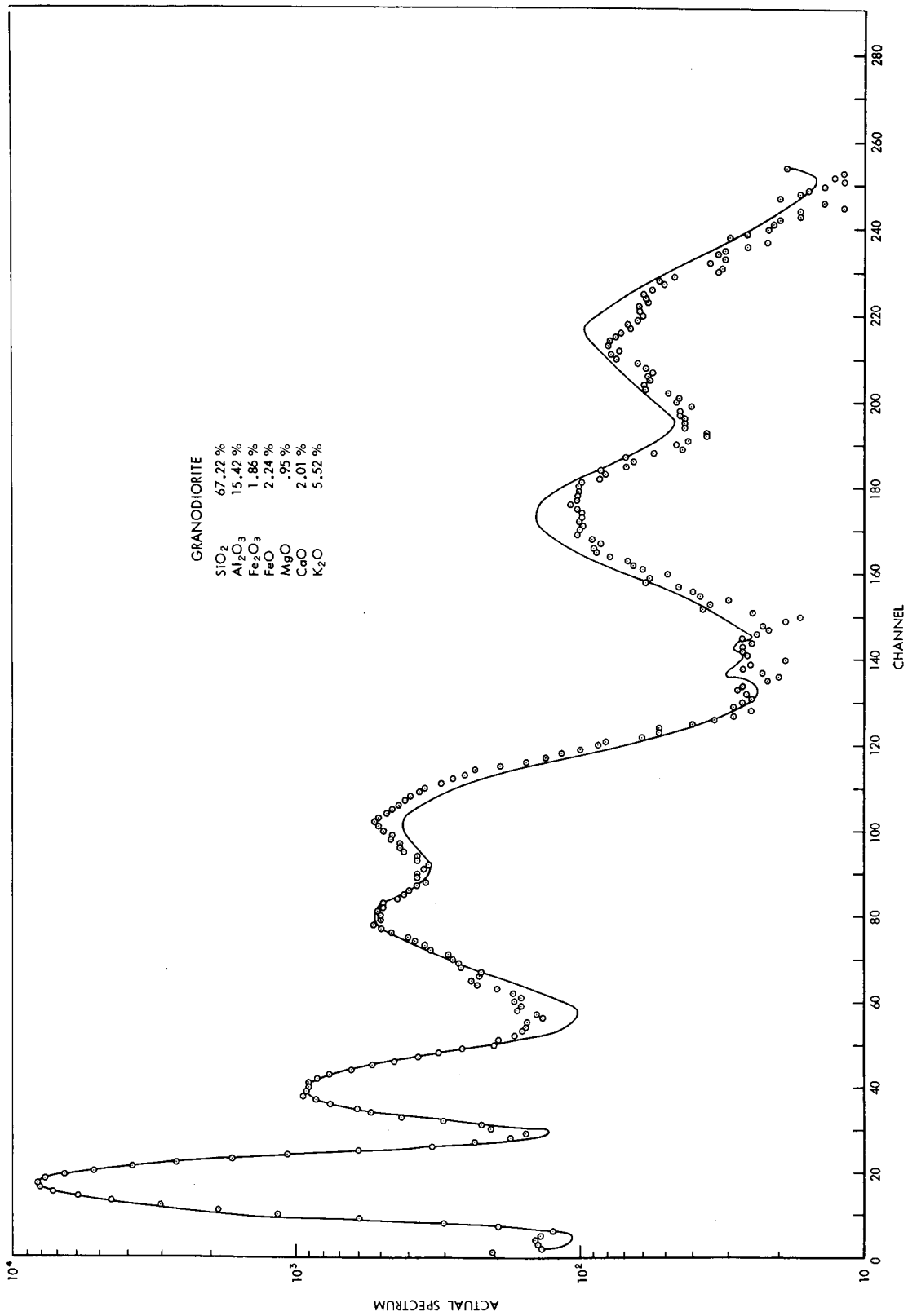


Figure 14

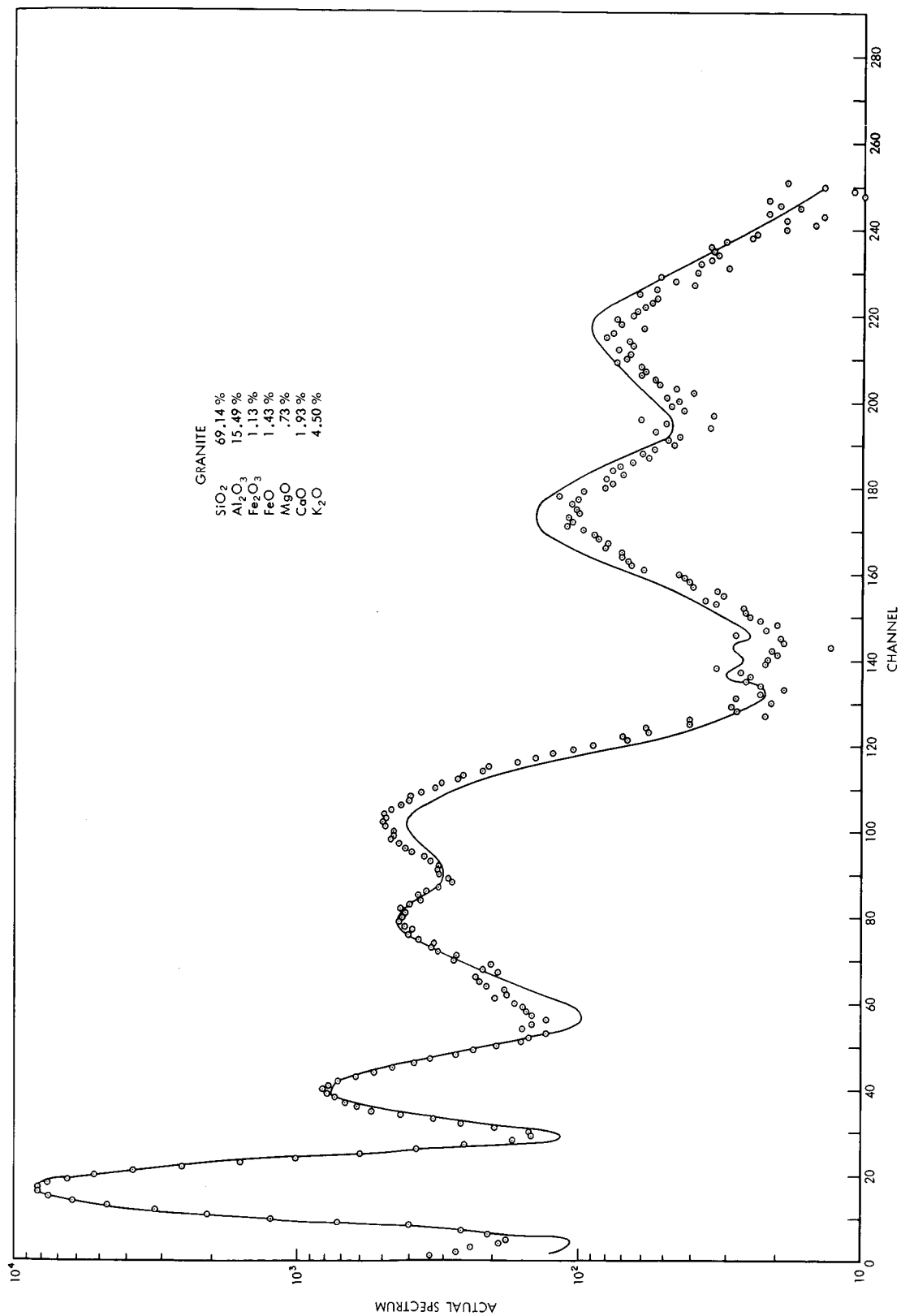


Figure 15

where one observes a number of discrete lines in the background spectrum, there is a slight divergence, very likely due to the difference in scattering between the samples measured and the boric acid pellet. These divergences shown in Figures 10-15 would actually appear smaller if the statistical spread for the data points were plotted (see Figure 6). Nevertheless these differences are real and do increase the statistical error in the determination of the relative intensities. These increased errors are reflected in an increase of  $\chi^2_i$ . The increase on the variance  $\sigma^2(\beta_\lambda)$  due to increase in  $\chi^2_i$  is then given by equation (13a) above.

In order to produce the synthesized curves shown in Figures 10-15, the relative intensities of each of the library components has been determined by using the least square criteria and the non-negativity constraint. These relative intensities are shown in Table I together with the statistical error. Blank portions in the table indicate components showing negative or zero intensity values. These are automatically rejected in the analysis and not included as part of the library. This is an indication that a particular component is either absent or its intensity contribution is indistinguishable statistically from the noise. The actual composition for each sample is shown in the corresponding figure (10-15). The percentage interference between elements (i.e., those greater than 10%) are given in Table II. It can be seen that the elements fall into three groups where interference is strong. These are: (1) Si, Mg, Al, (2) Ca, K, and (3) Fe, Mn. In these groups, unless an additional constraint is used such as that described below, it is very difficult to determine the concentrations of the individual components even though the sums of the relative intensities are correct.

Table I  
Relative Intensities Obtained from the Least Squares Analysis

Element	Rock Type					
	Dunite	Peridotite	Basalt	Andesite	Granodiorite	Granite
Si	.26 × 10 <sup>5</sup> ± .006 × 10 <sup>5</sup>	.25 × 10 <sup>5</sup> ± .006 × 10 <sup>5</sup>	.41 × 10 <sup>5</sup> ± .009 × 10 <sup>5</sup>	.50 × 10 <sup>5</sup> ± .008 × 10 <sup>5</sup>	.56 × 10 <sup>5</sup> ± .008 × 10 <sup>5</sup>	.56 × 10 <sup>5</sup> ± .01 × 10 <sup>5</sup>
Corrected Value*	.301 × 10 <sup>5</sup> ± .018 × 10 <sup>5</sup>	.30 × 10 <sup>5</sup> ± .017 × 10 <sup>5</sup>	.47 × 10 <sup>5</sup> ± .011 × 10 <sup>5</sup>	.52 × 10 <sup>5</sup> ± .012 × 10 <sup>5</sup>		
Al	.18 × 10 <sup>4</sup> ± .08 × 10 <sup>4</sup>	.30 × 10 <sup>4</sup> ± .07 × 10 <sup>4</sup>	.13 × 10 <sup>5</sup> ± .009 × 10 <sup>5</sup>	.13 × 10 <sup>5</sup> ± .009 × 10 <sup>5</sup>	.12 × 10 <sup>5</sup> ± .006 × 10 <sup>5</sup>	.13 × 10 <sup>5</sup> ± .01 × 10 <sup>5</sup>
Corrected Value*	0	0	.721 × 10 <sup>4</sup> ± .085 × 10 <sup>4</sup>	.111 × 10 <sup>5</sup> ± .014 × 10 <sup>5</sup>	.105 × 10 <sup>5</sup> ± .013 × 10 <sup>5</sup>	.780 × 10 <sup>4</sup> ± .093 × 10 <sup>4</sup>
Fe	.13 × 10 <sup>5</sup> ± .005 × 10 <sup>5</sup>	.12 × 10 <sup>5</sup> ± .005 × 10 <sup>5</sup>	.14 × 10 <sup>5</sup> ± .006 × 10 <sup>5</sup>	.79 × 10 <sup>4</sup> ± .05 × 10 <sup>4</sup>	.40 × 10 <sup>4</sup> ± .04 × 10 <sup>4</sup>	.24 × 10 <sup>4</sup> ± .05 × 10 <sup>4</sup>
Mg	.12 × 10 <sup>5</sup> ± .005 × 10 <sup>5</sup>	.89 × 10 <sup>4</sup> ± .04 × 10 <sup>4</sup>	.47 × 10 <sup>3</sup> ± .39 × 10 <sup>3</sup>	.28 × 10 <sup>3</sup> ± .33 × 10 <sup>3</sup>		.93 × 10 <sup>3</sup> ± .42 × 10 <sup>3</sup>
Corrected Value*	.972 × 10 <sup>4</sup> ± .12 × 10 <sup>4</sup>	.74 × 10 <sup>4</sup> ± .08 × 10 <sup>4</sup>	.252 × 10 <sup>4</sup> ± .151 × 10 <sup>4</sup>	.94 × 10 <sup>3</sup> ± .99 × 10 <sup>3</sup>	.194 × 10 <sup>4</sup> ± .149 × 10 <sup>4</sup>	.364 × 10 <sup>4</sup> ± .280 × 10 <sup>4</sup>
Ca	.33 × 10 <sup>3</sup> ± .20 × 10 <sup>3</sup>	.67 × 10 <sup>3</sup> ± .19 × 10 <sup>3</sup>	.75 × 10 <sup>4</sup> ± .03 × 10 <sup>4</sup>	.58 × 10 <sup>4</sup> ± .04 × 10 <sup>4</sup>	.31 × 10 <sup>4</sup> ± .03 × 10 <sup>4</sup>	.30 × 10 <sup>4</sup> ± .03 × 10 <sup>4</sup>
K	.49 × 10 <sup>2</sup> ± 1.8 × 10 <sup>2</sup>	.18 × 10 <sup>3</sup> ± .17 × 10 <sup>3</sup>	.38 × 10 <sup>4</sup> ± .04 × 10 <sup>4</sup>	.50 × 10 <sup>4</sup> ± .03 × 10 <sup>4</sup>	.76 × 10 <sup>4</sup> ± .04 × 10 <sup>4</sup>	.61 × 10 <sup>4</sup> ± .04 × 10 <sup>4</sup>
Ti	.55 × 10 <sup>3</sup> ± .14 × 10 <sup>3</sup>	.50 × 10 <sup>3</sup> ± .13 × 10 <sup>3</sup>	.18 × 10 <sup>4</sup> ± .02 × 10 <sup>4</sup>	.81 × 10 <sup>3</sup> ± .18 × 10 <sup>3</sup>		
Mn	.39 × 10 <sup>4</sup> ± .03 × 10 <sup>4</sup>	.37 × 10 <sup>4</sup> ± .04 × 10 <sup>4</sup>	.33 × 10 <sup>4</sup> ± .05 × 10 <sup>4</sup>	.16 × 10 <sup>4</sup> ± .04 × 10 <sup>4</sup>	.10 × 10 <sup>4</sup> ± .04 × 10 <sup>4</sup>	.10 × 10 <sup>4</sup> ± .04 × 10 <sup>4</sup>

\*Corrected values are those with interference removed.

Table II  
Correlation Greater Than 10% between  
Library Components

	Si	Al	Fe	Mg	Ca	K	Ti	Mn	Back
Si		45%		16%					
Al				55%					
Fe								42%	
Mg									
Ca						40%			
K									
Ti									
Mn									
Back									

#### B. Resolving Correlations

We now shall consider the case of the Si-Al-Mg correlation in detail. As indicated above, another physical constraint is required in order to resolve the interferences. Since aluminum has a strong absorption edge lying between the silicon and the aluminum K lines, a 0.5 mil aluminum foil was used in front of the detector window to preferentially absorb the silicon K radiation. Figures 16 and 17 show for example the pulse height spectra of the dunite and granite taken under these conditions. In comparison to the spectra for these rocks



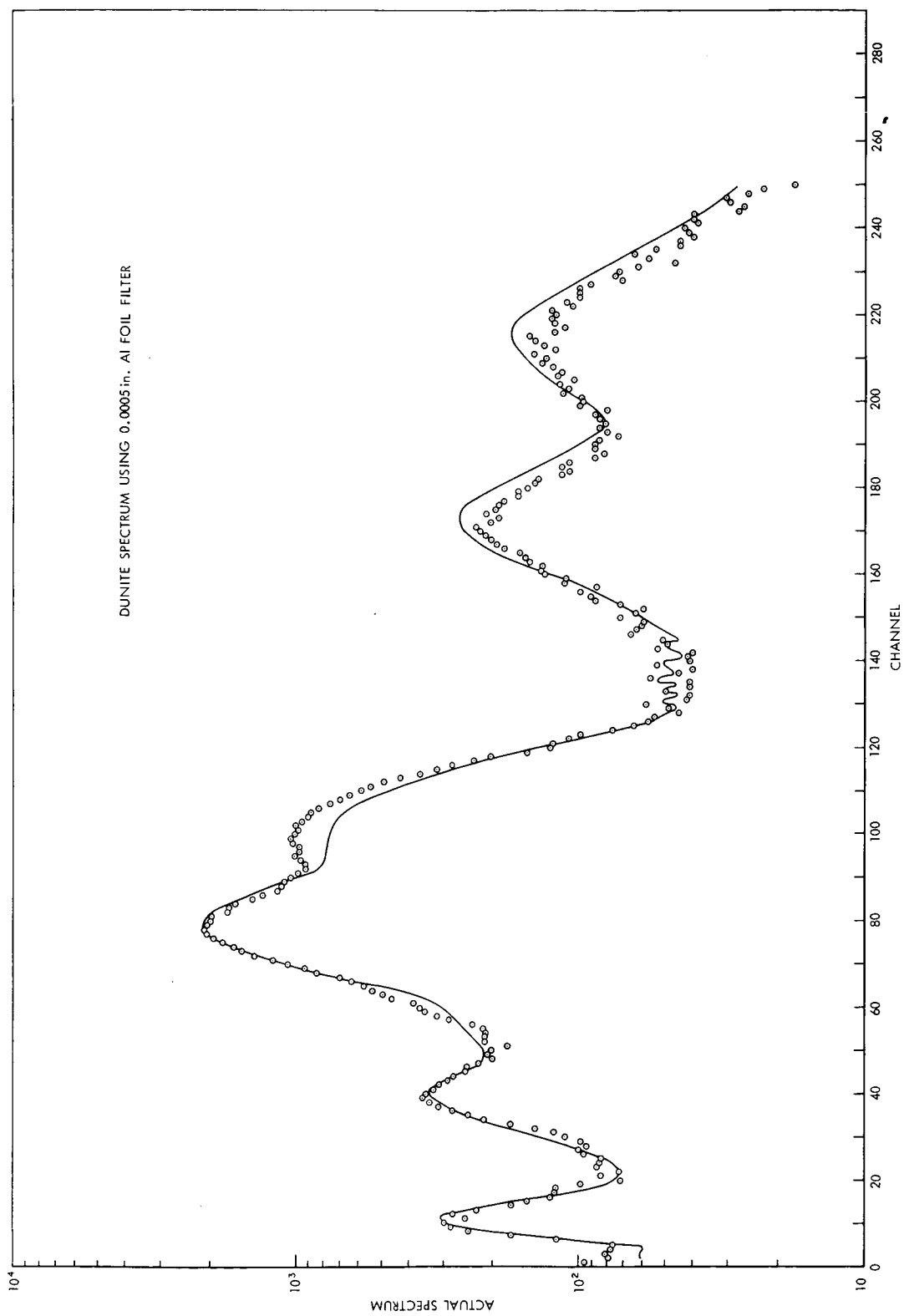


Figure 16

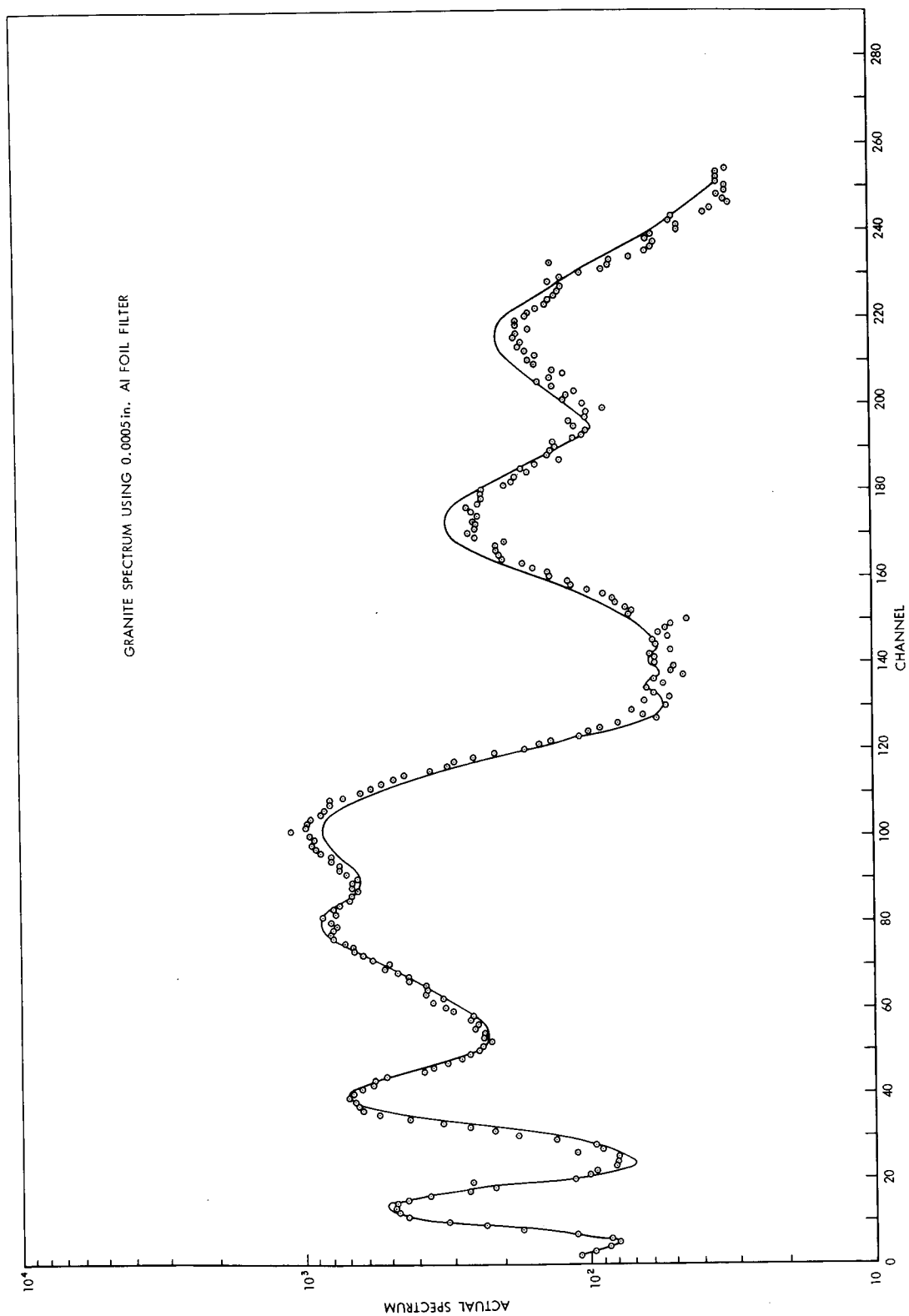


Figure 17

Table III

Results Obtained for Plan View Meteorite Using the Least Squares Analysis

Element	Relative Intensities from Least Squares Analysis	% Composition from Fig. 17	Reported Chemical Analysis*
Fe	$.36 \times 10^5 \pm .02 \times 10^5$	$14.1 \pm 2.8$	17.-24.
Si	$.31 \times 10^5 \pm .01 \times 10^5$	$17.5 \pm .7$	17.25
Al	$.25 \times 10^4 \pm .09 \times 10^4$	$3.2 \pm 1.5$	1.08
Mg	$.54 \times 10^4 \pm .05 \times 10^4$	$18. \pm 2.5$	13.71
Ca	$.24 \times 10^4 \pm .03 \times 10^4$	$1.08 \pm .21$	1.19
K	$.95 \times 10^3 \pm .30 \times 10^3$	$.1 \pm .03$	.066

\*Quarterly Rept of the U.S. Geological Survey, April-June 1965.

previously shown in Figures 10 and 15 the dunite now shows a distinct Mg peak and the Al line is predominant in the granite.

The least square analysis technique using a non-negativity constraint and an aluminum foil filter was applied to the same suite of six rocks shown in Figures 10-15. Because of the strong silicon absorption, the silicon component was eliminated from the analysis. The relative intensities of the Al and Mg obtained were corrected for absorption due to the Al filter. While a strong correlation is possible between these elements, this was not a significant factor in this instance because where the Mg concentration was high, the Al concentration was very low and vice-versa.

If Al and Mg were both present in large amounts or if it is required that the Al and Mg be known with great accuracy, then an magnesium filter could be used to selectively absorb the Al radiation, and resolve this correlation.

Since the Al and Mg relative intensities had been determined, these components were then stripped out of the original spectrum and the Si relative intensity determined using Flow 1 of the computer program. These results are listed in Table I as corrected values for Si, Al and Mg and can be compared to the uncorrected values within the same block.

Figure 18 is a plot on a log-log scale of the relative intensities versus chemical composition for Si, Al, Mg, K, Ca and Fe. The solid lines are least square fits to the data points obtained from the computer analysis. There is a good approximation to a linear relationship between relative intensity and percentage composition, consistent with the small concentration range. No line was drawn for the Mg because the lower Mg concentrations are associated with high Al concentrations in these samples and the strong correlation between these two elements makes it difficult to determine the Mg component without very large errors. It is significant that one can easily distinguish between a 10% relative concentrational variation in the 30% range. The error bars in these plots are strictly fluctuations due to counting statistics and background correction. These can be partially reduced by increased counting times and background reduction.

### C. Classification of Rock Types

Although the curves in Figure 18 show a reasonable linear approximation between relative intensity and concentration one does not intend to infer that this method can yield precise chemical analysis. No attempt has been made at careful sample preparation or to correct for matrix effects such as absorption or

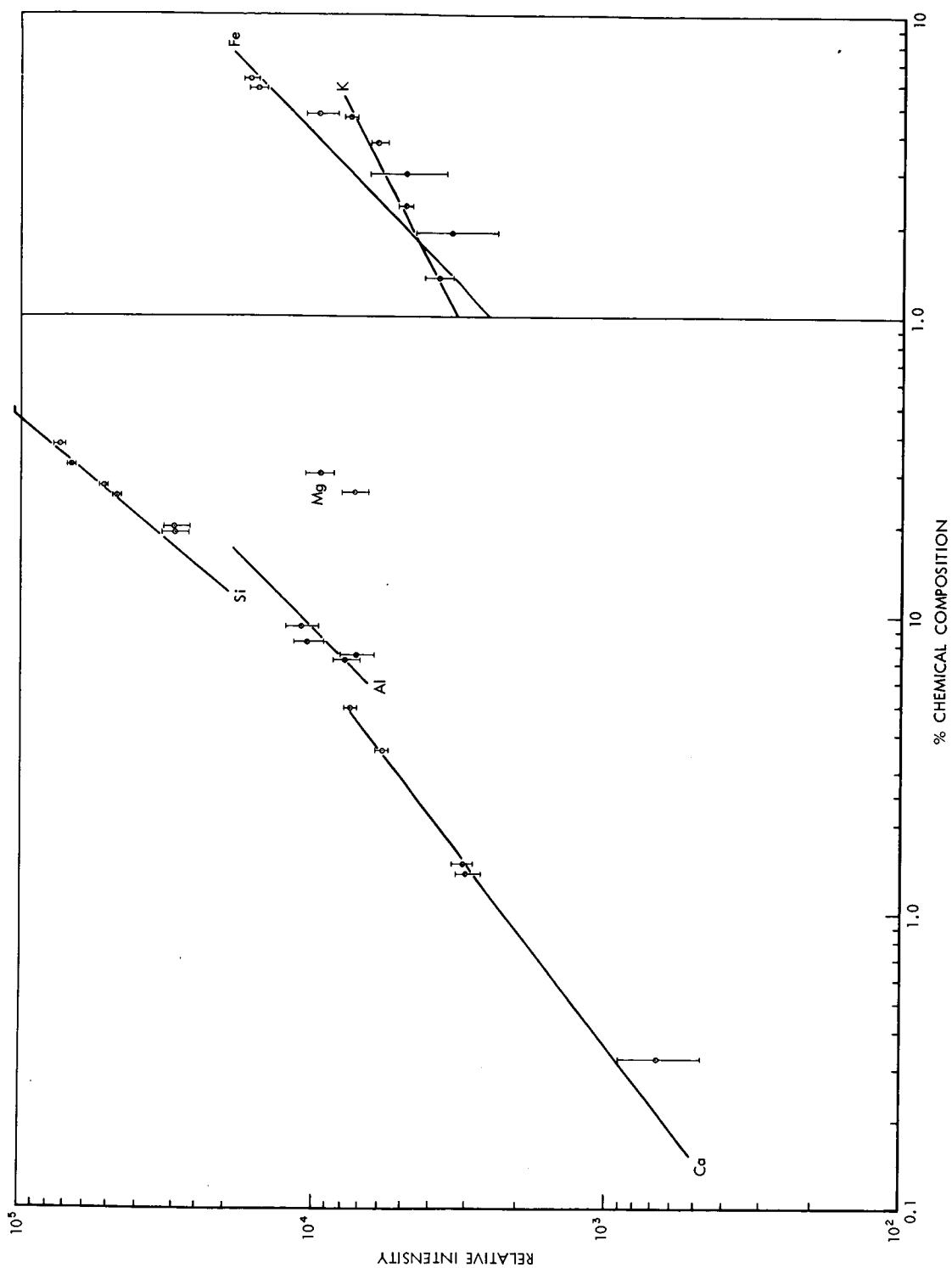


Figure 18

enhancement. In fact, in terms of a lunar surface mission, a serious attempt has been made to determine how much chemical information can be obtained without careful control above factor. Using these ground rules the data will be used in an attempt at broad classification of rock types. The approach is similar to those in the studies performed using neutron methods described in references 25-29.

A preliminary classification of the rocks according to type is made on the basis of the presence or absence of certain chemical elements simply determined from the computer output, for example the presence or absence of large amounts of Mg, Al, Ca and K. For example the ultra-basic rocks are rich in Mg with negligible amounts of Al, Ca and K (see Table I and Figures 10-15).

Following this, an approach similar to that described for the neutron-gamma techniques (references 25-29) is used. Rather than attempting to carefully control the sample geometry, ratios of various elements have been calculated as shown in Figures 19-25. One observes again a good approximation to a linear relationship between chemically determined and calculated ratios. As pointed out by Waggoner (reference 29) it is obvious that no one element or ratio of elements can be used to classify a rock type. However, if one combines a number of these factors, then it is possible to categorize a rock as lying somewhere on the scale between the ultra-basic and acidic rocks. This can, of course, only be done to the extent that a chemical analysis is meaningful in this context.

#### D. Quantitative Analysis

The performance of quantitative analysis normally requires extreme care in sample preparation, the use of appropriate standards and adjustment for matrix effects. Such requirements are sometimes difficult to fulfill even in a

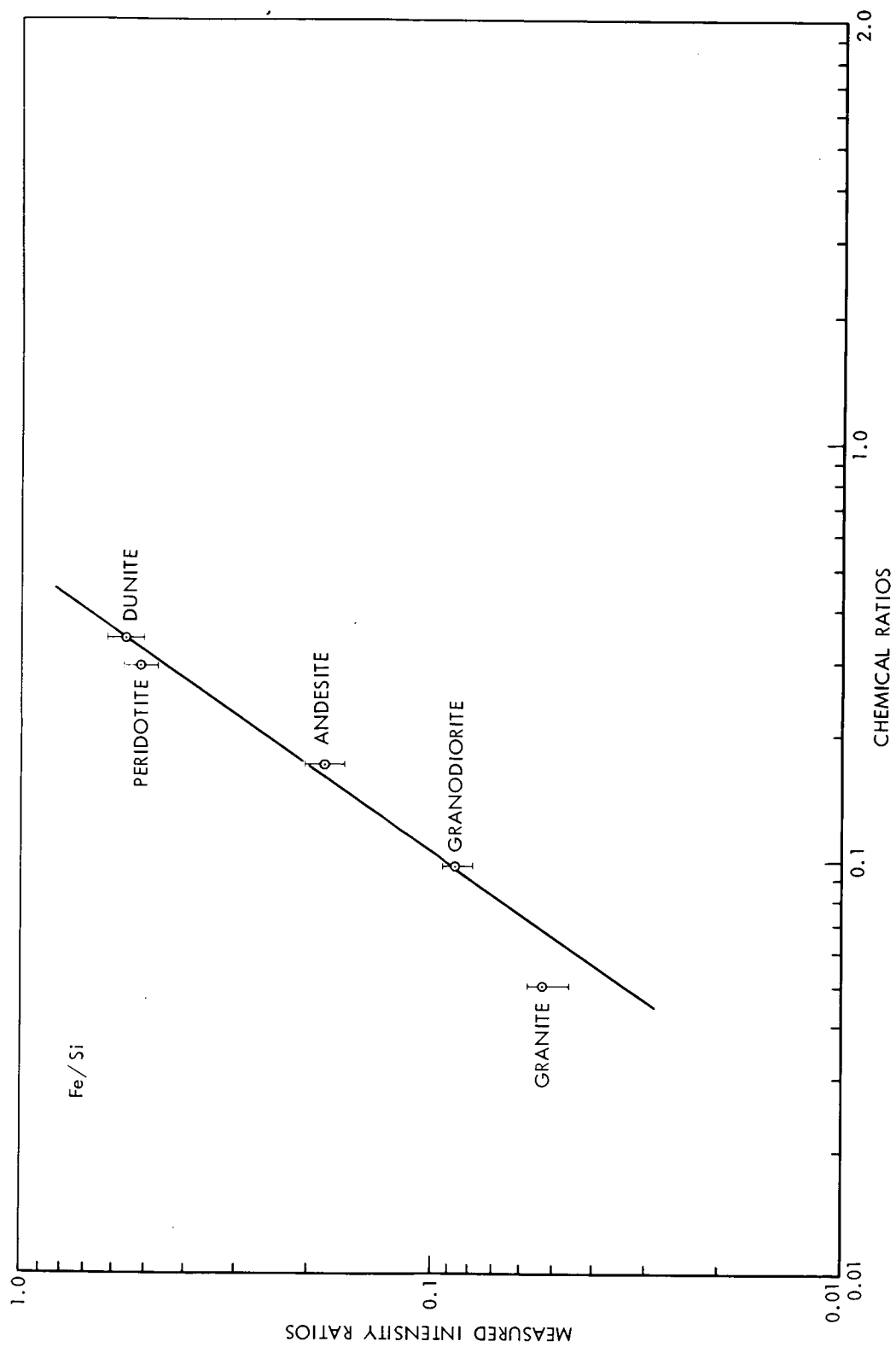


Figure 19

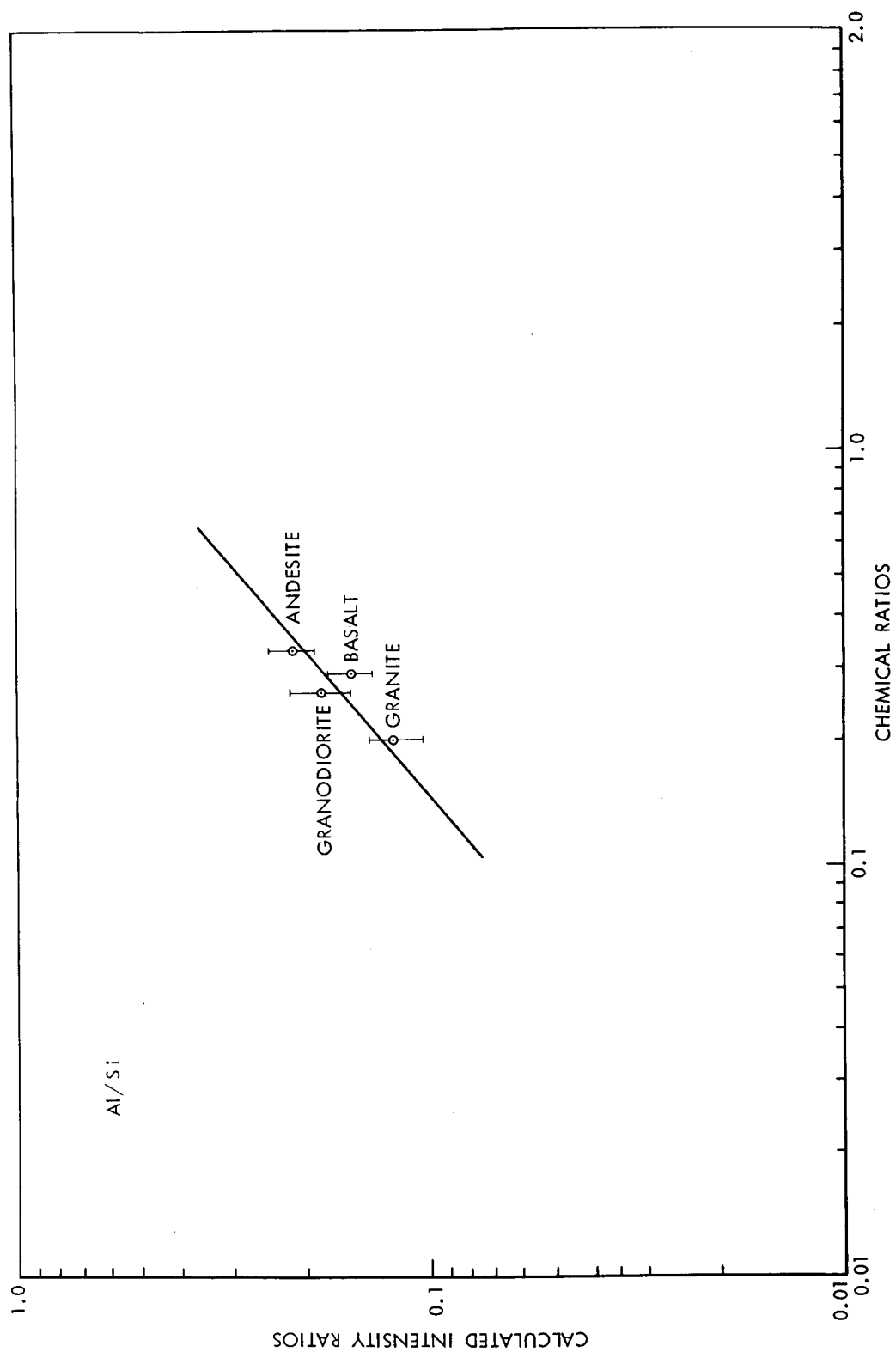


Figure 20



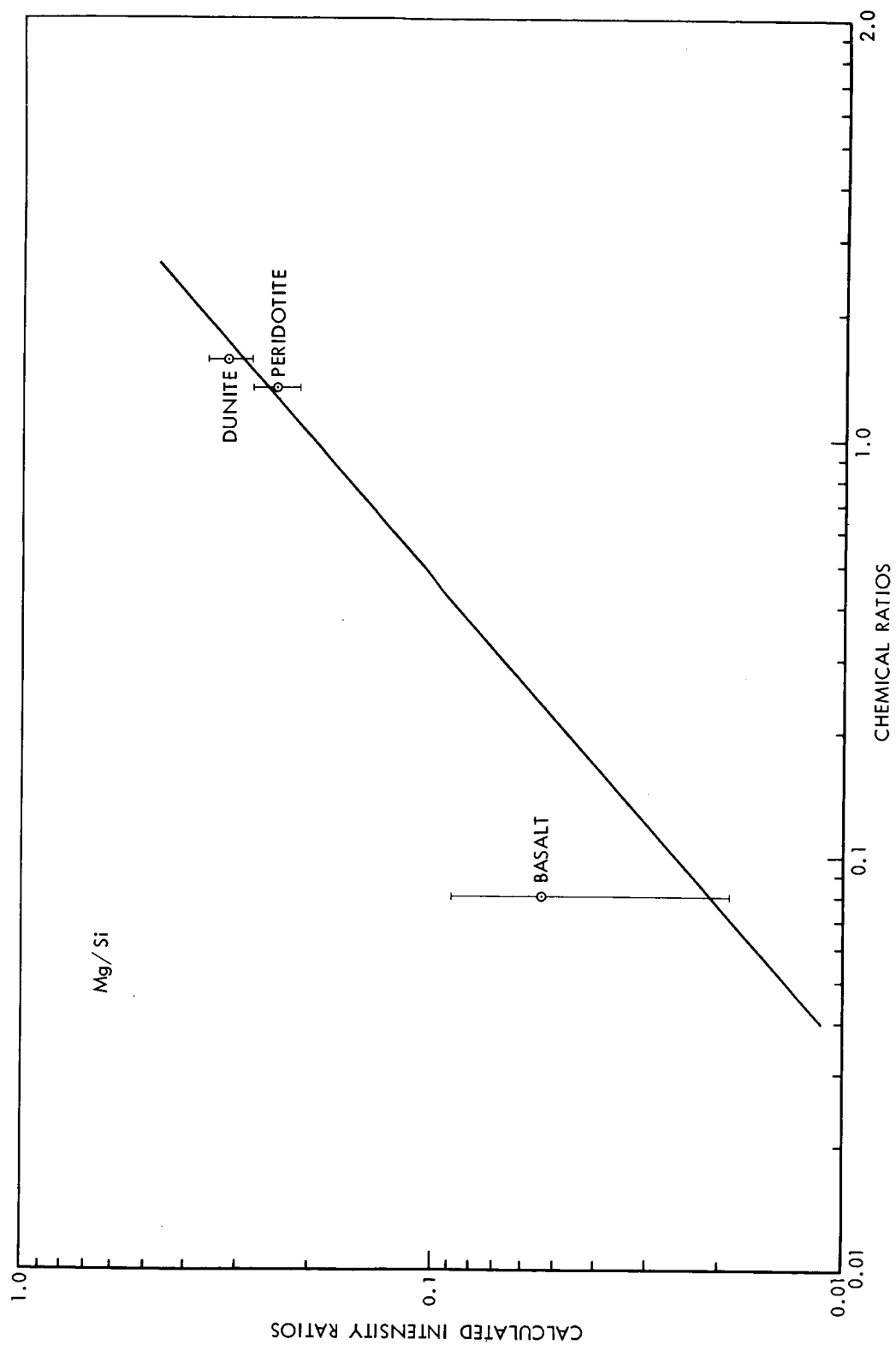


Figure 21

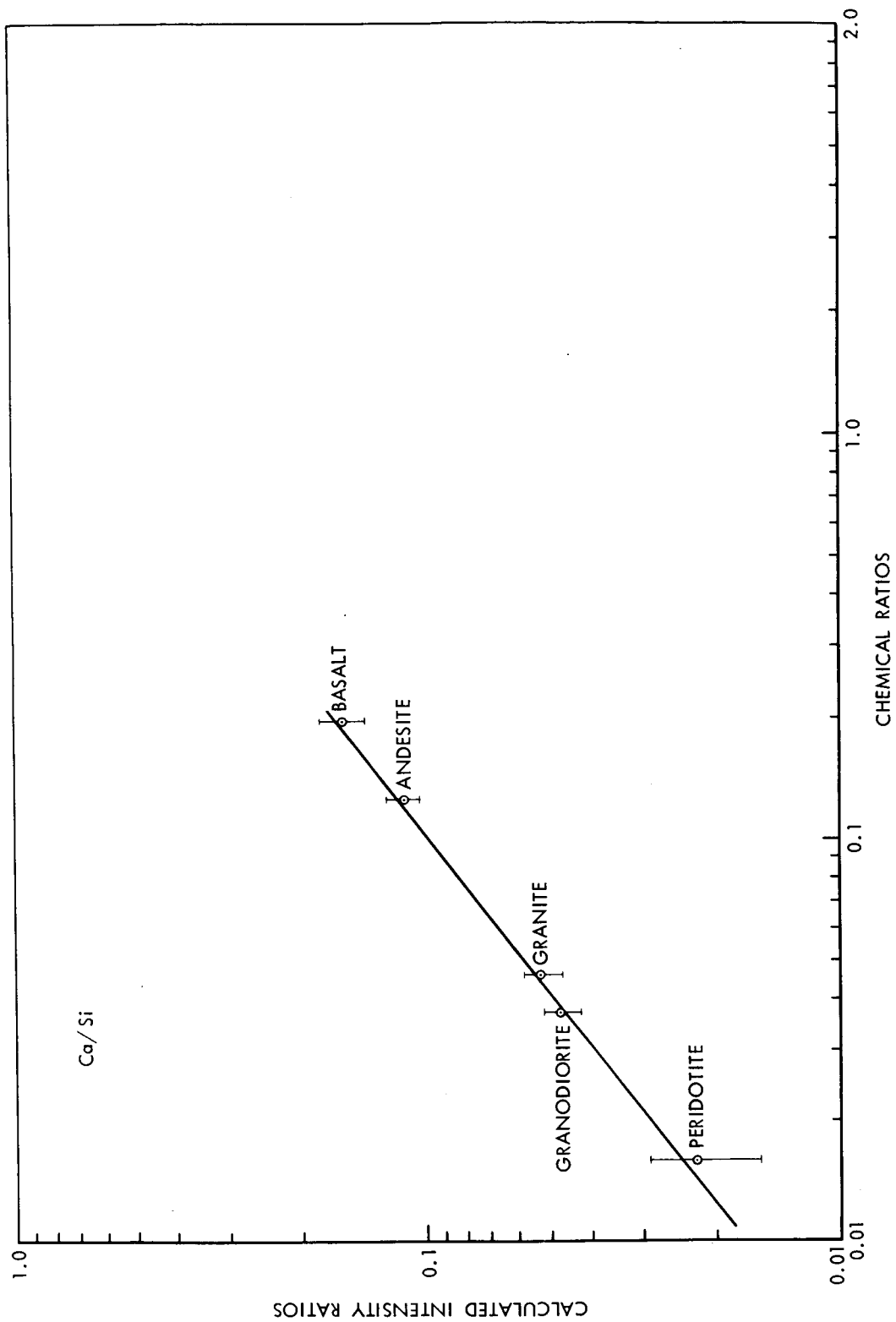


Figure 22

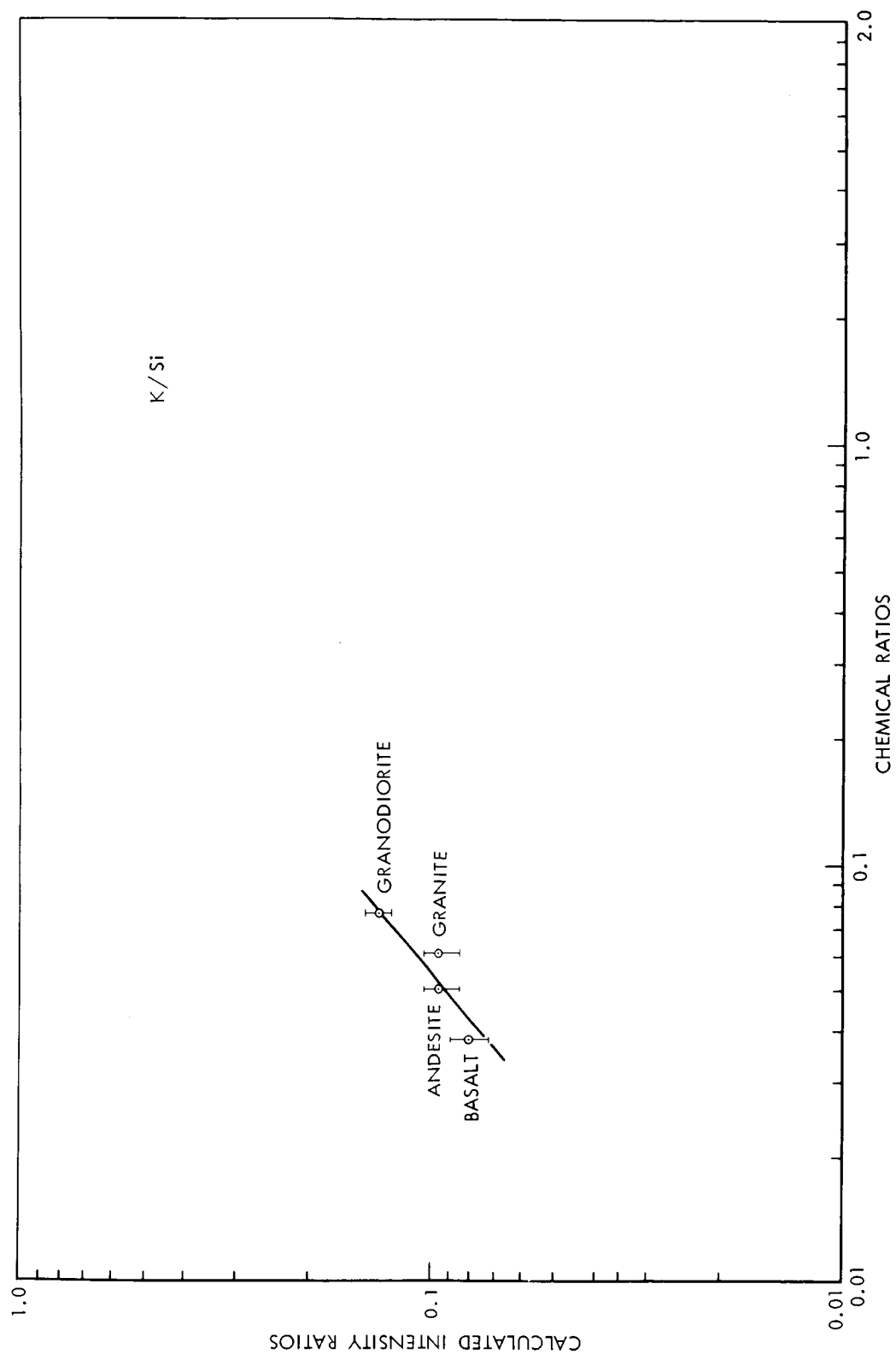


Figure 23

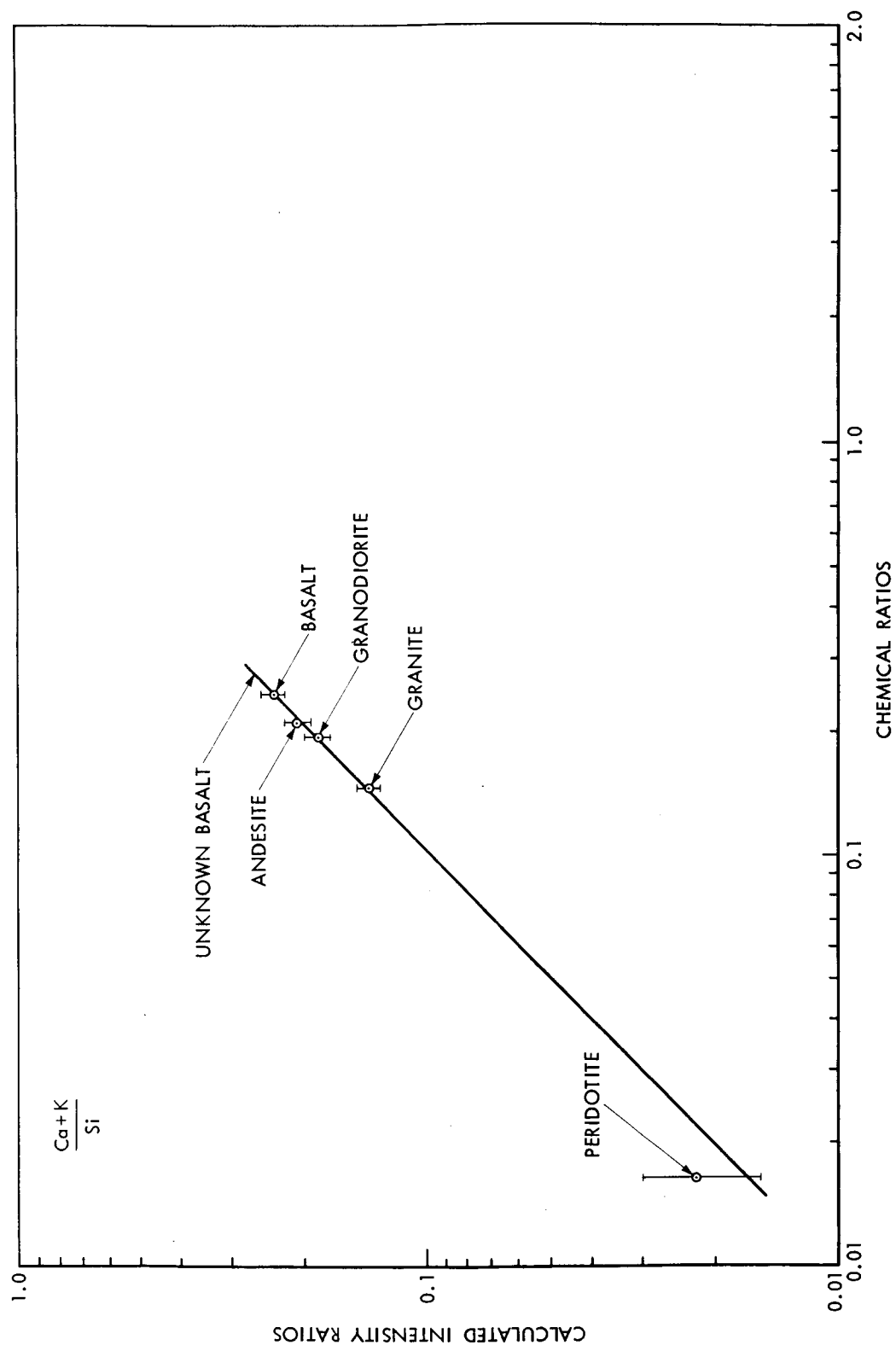


Figure 24

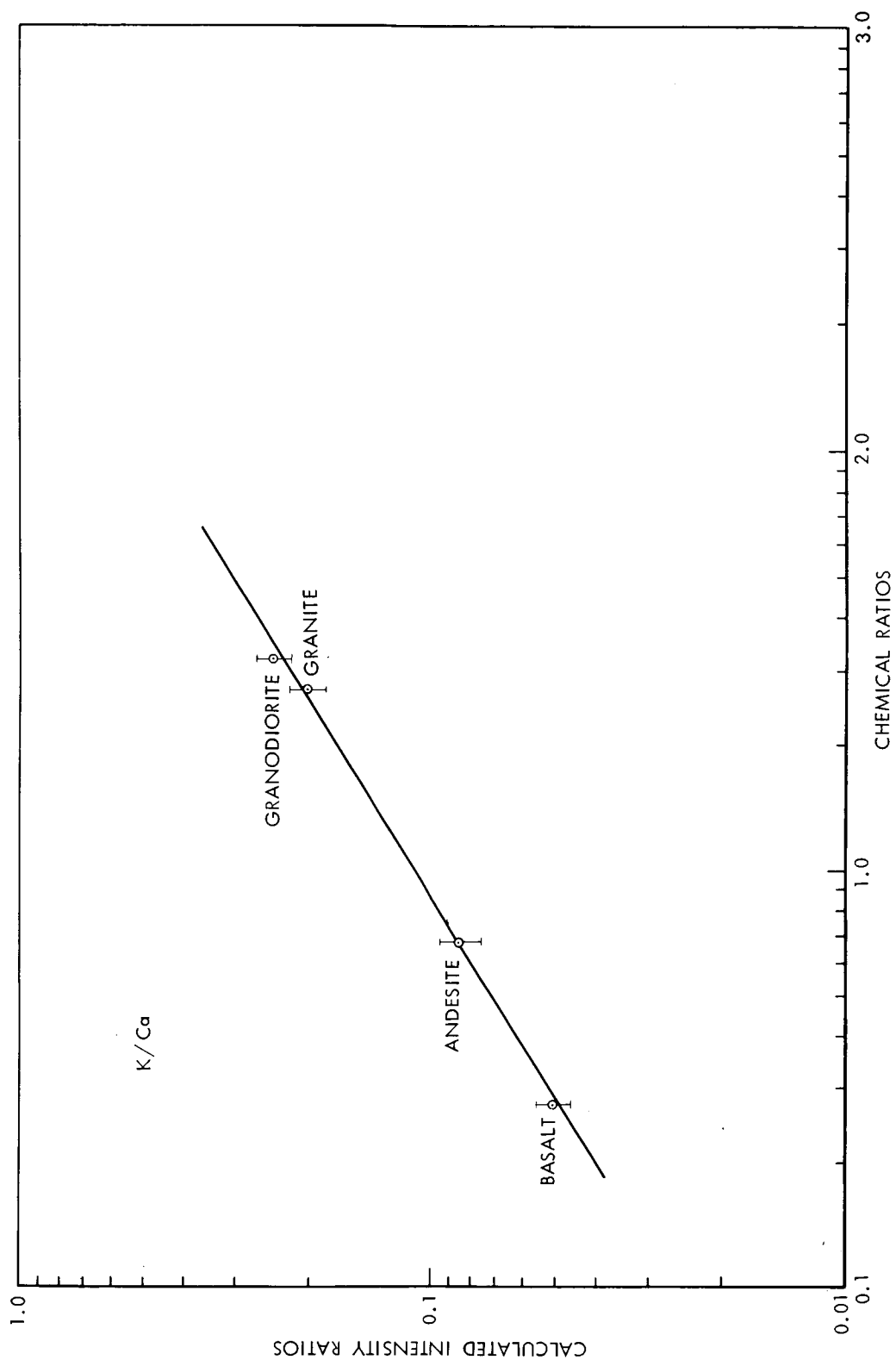


Figure 25

laboratory environment. One cannot even hope to control these parameters in a remote exploration program. Keeping these constraints in mind, an attempt was made, using these rough procedures to perform an analysis on a meteorite to obtain some idea of the possibility for performing a quantitative analysis.

Figure 26 shows the measured pulse height spectrum obtained for the Plainview Meteorite, a bronzite-chondrite. Table III summarizes the results obtained using the curves of Figure 17 as calibration curves. The agreements can be considered as quite satisfactory for a first cut chemical analysis. These results combined with the data used to prepare the calibration curves show that one can expect to obtain useful chemical values, satisfying the goals for a lunar geo-chemical exploration device.

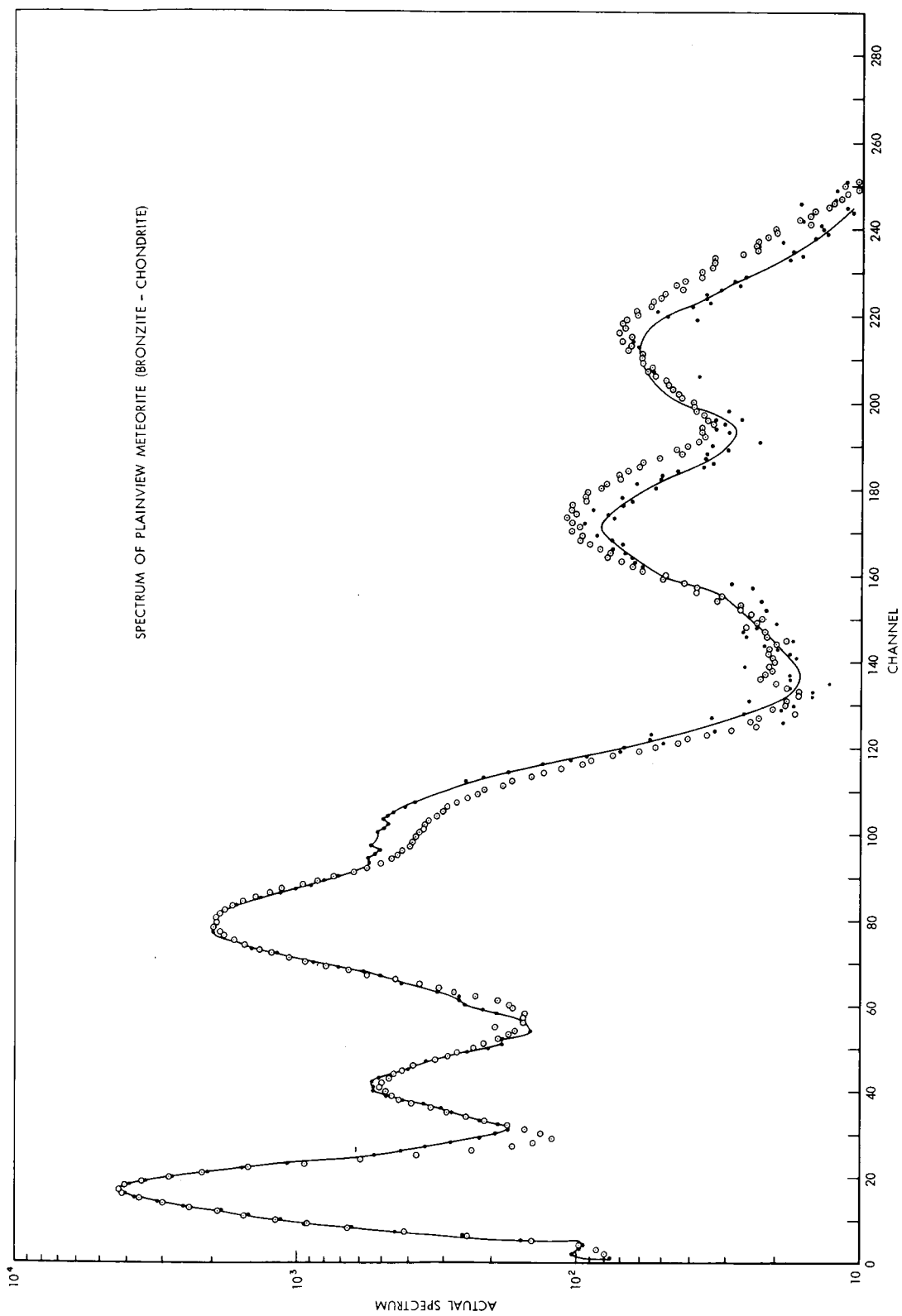


Figure 26

## REFERENCES

1. A. E. Metzger, R. E. Parker, and J. I. Trombka, "A Non-dispersive X-ray Spectrometer for Lunar and Planetary Geochemical Analysis," IEE Trans. Nuclear Science, Volume NS-13, No. 1, February, 1966.
2. B. Sellers and C. A. Zieger, "Radioisotope Alpha Excited Characteristic X-ray Sources," presented at symposium on Low Energy X and Gamma Sources and Applications, Chicago, Illinois, October 1964. Proceedings published by U.S.A.E.C.
3. J. O. Karttunen, et al., "A Portable Fluorescent X-ray Instrument Utilizing Radioisotope Sources," Anal. Chem. 36, 1277 (1964).
4. J. I. Trombka and I. Adler, "Analytic Method for a Non-Dispersive Analysis" presented at "The First National Conference on Electron Probe Micro-analysis," University of Maryland, College Park, Md., May 1966.
5. J. F. Cameron and J. R. Rhodes, "Beta-excited Characteristic X-rays as Energy Reference Sources," International Journal of Applied Radiation and Isotopes, Vol. 7, pp. 244-250, (1960).
6. J. F. Cameron and J. R. Rhodes, "X-ray Spectrometry with Radioactive Sources," Nucleonics, Vol. 19, No. 6, pp. 53-57, June 1961.



7. A. Robert, "Contributions to the Analysis of Light Elements Using X-Fluorescence Excited by Radioelements," Commissariat a l'Energie Atomique, Rapport CEA-R2539, 1964.
8. H. Friedman, Advances in Spectroscopy, edited by Thomson, John Wiley and Sons, 1964.
9. A. Robert and P. Martinelli, "Method of Radioactive Analysis of Heavy Elements by Virtue of X-ray Fluorescence," Paper No. SM 55/76 at IAEA Meeting, Salzburg, Austria, October 1964.
10. H. Imamura, K. Vehida and H. Tominaya, "Fluorescent X-ray Analyser, with Radioactive Sources for Mixing Control of Cement Raw Materials," Radioisotopes, Vol. 11, No. 4, July 1965.
11. S. C. Curran, "The Proportional Counter as Detector and Spectrometer, Hendbuch der Physik, Bd. XLV, Springer-Verlag, Berlin-Gottingen, Heidelberg, 1958.
12. J. I. Trombka, "Least-squares Analysis of Gamma-ray Pulse Height Spectra," NAS-NS-3107, pp. 183-201, March 1963.

13. W. R. Burrus, "Unscrambling Scintillation Spectrometer Data," IRE Transactions on Nuclear Science, Vol. INS-7, No. 23, February, 1960.
14. M. E. Rose, "The Analysis of Angular Correlation and Angular Data," The Physical Review, Vol. 91, p. 610, 1953.
15. W. A. Hestin, R. L. Heath, R. D. Helmer, "Quantitative Analysis of Gamma Ray Spectras by the Method of Least Squares, IDO-16781, June 15, 1962.
16. R. L. Heath, "Data Analysis Techniques for Scintillation Spectrometry," IDO-16784, May 29, 1962.
17. Schoenfeld, private communication.
18. A. Turkivitch and E. Franzrote, private communication.
19. E. Beale, "On Quadratic Programming," Naval Research Logistics Quarterly, Vol. 6, September 1959.
20. H. Scheffe, The Analyses of Variance, John Wiley and Sons, Inc., New York, 1959.
21. C. A. Bennett and H. L. Franklein, Statistical Analysis in Chemistry and the Chemical Industry, John Wiley and Sons, Inc., New York, 1954.

22. P. Poulson, R. Parker, and J. I. Trombka, Computer Program Report,  
"Linear Least Square Analysis of Radiation Spectra," Interoffice Memo,  
Jet Propulsion Laboratory, March 31, 1965.
23. J. I. Trombka, "On the Analysis of Gamma Ray Pulse Height Spectra,"  
Dissertation, Univ. of Michigan, 1962.
24. J. I. Trombka, A. Metzger, "Neutron Method for Lunar and Planetary  
Surface Compositional Studies," Analysis Instrumentation 1963, edited by  
L. Fouler, R. D. Eanes, and T. J. Kehoe, Plenum Press, New York, 1963.
25. C. D. Schroder, J. A. Waggoner, J. A. Bengert, E. F. Martina and R. J.  
Stinner, "Neutron-Gamma Ray Instrumentation for Lunar Surface  
Composition Analyses," ARS Journal, 32, 631, 1962.
26. R. C. Greenwood and J. H. Reed, "Scintillation Spectrometer Measurements  
of Captured Gamma Rays from Natural Elements," Proceedings of the 1961  
International Conference of Modern Trends in Activation Analysis, A and M  
College of Texas, 1961.

27. L. E. Fite, E. L. Steele, and R. E. Wainerdi, "An Investigation of Computer Coupled Automatic Activation Analysis and Remote Lunar Analyses," Quarterly Report, TID-18257, 1963.
28. A. E. Metzger, "Some Calculations Bearing on the Use of Neutron Activation for Remote Compositional Analysis," Jet Propulsion Laboratory Technical Report No. 32-386, Jet Propulsion Laboratory, Pasadena, California, August, 1962.
29. J. A. Waggoner and R. J. Knox, "Elemental Analysis Using Neutron Inelastic Scatter," UCRL-14654-T.

## LIST OF ILLUSTRATIONS

1.  $\alpha$  source x-ray analyzer
2.  $\alpha$  emitter source holder
3. Background pulse height spectrum:  $\text{cm}^{242}$  source; boric acid scatterer; a 90% A, 10%  $\text{CH}_4$ , .001" Be window proportional counter.
4. Counter tube efficiency: 90% A, 10%  $\text{CH}_4$  filling; .001 in Be window; 2 cm absorption path.
5. Discrete energy spectrum and corresponding pulse spectrum of the characteristic Fe x-ray lines. Pulse height spectrum measured with a sealed 90% A, 10%  $\text{CH}_4$  proportional counter.
6. Pulse height spectrum of basalt measured with a proportional counter filled with 90A and 10%  $\text{CH}_4$ . The following can be seen: (1) The monoelemental components; (2) The envelope due to the sum of the monoelemental components; and (3) The measured pulse height spectrum with statistical variations included.
7. Percentage of interference for various resolutions.
8. The effect of gain shift on silty sand from Hoppe Butte, Arizona.
9. Flow diagrams for least squares analysis.
10. Pulse height spectrum of dunite.

11. Pulse height spectrum of peridotite.
12. Pulse height spectrum of Basalt.
13. Pulse height spectrum of andesite.
14. Pulse height spectrum of grandiorite.
15. Pulse height spectrum of granite.
16. Dunite spectrum with 1/4 mil aluminum absorber.
17. Granite spectrum with 1/2 mil aluminum absorber.
18. Measured relative intensity as a function of chemical composition.
19. Measured Fe/Si intensity ratios versus chemical composition.
20. Measured Al/Si intensity ratios versus chemical composition.
21. Measured Mg/Si intensity ratios versus chemical composition.
22. Measured Cu/Si intensity ratios versus chemical composition.
23. Measured K/Si intensity ratios versus chemical composition.
24. Measured (Cu + K)/Si intensity ratios versus chemical composition.
25. Measured K/Cu intensity versus chemical composition.
26. Spectrum of Planvie Meteorite (bronze).